Geotechnical
Information Center

Lead Distribution and Availability in Contaminated Soils at the Abandoned Cuba Smelter Site, Socorro, New Mexico

By

Christopher P. Wolf

Submitted in Partial Fulfillment of the Requirements for the Degree of
Master in Science in Geochemistry
New Mexico Institute of Mining and Technology
Socorro, New Mexico

ABSTRACT

Availability and distribution of lead (Pb) in soils were investigated at the Cuba smelter site in Socorro, New Mexico. The Cuba Smelter was active from 1881 until the start of World War I (about 1915) and processed Pb ores from mining districts near Socorro. The site was deemed a potential health hazard by the state of New Mexico in 1990. In 1991, an X-ray fluorescence (XRF) study determined that soils exceeded the EPA action level of 500 parts per million (ppm) Pb, so a remedial clean-up occurred which was completed in 1994.

Availability and distribution of Pb in soils are used to predict potential health threats. Availability is a qualitative term used to describe what fraction of Pb in a system will react with soil solutions, gastrointestinal fluids, or groundwater. A more specific availability term is bioavailability which is a measure of absorption and utilization by an organism (plants and animals). Distribution describes Pb partitioning between grain sizes.

Physical and chemical parameters were determined for soils collected adjacent to the former smelter foundation on a natural terrace (CS-I) and from a fallow agricultural field directly east of the smelter (CS-II). These two areas had elevated Pb levels determined during the XRF survey by EPA contractors. Slag samples were collected from near the smelter foundation, also. Availability was evaluated by determining the mineralogy of Pb bearing phases and considering the solubility of the minerals in these soils. Pb distribution was determined using atomic absorption (AA) directly on bulk, sand, and clay fractions. Silt values were then calculated.

The grain-size is dominantly sand on the terrace and silt in the field. Soils are alkaline as indicated by pH values of 7.2 to 7.9 and negative values for net acid producing potentials (NAPP). Soil Pb concentrations range from 900 ppm to 9,600 ppm. Terrace samples have the highest Pb concentrations in the clay-size fraction, but the highest Pb concentrations in agricultural field samples are in the sand-size fraction. Pb-bearing phases identified include galena, chalcopyrite, pyrite, slag, and Pb-oxides. Minerals present in the soils were calcite, feldspars, quartz, and clay minerals. The clay minerals were illite, mixed layer illite/smectite (I/S), smectite, and kaolinite

Soil conditions at the Cuba smelter site reduced Pb availability. Sulfide minerals showed no signs of alteration. Galena was insoluble in the dry alkaline soils and did not oxidize to form anglesite armoring. Slag formed glassy rims surrounding eutectic textures of lead and copper sulfides and did not show signs of devitrification. Pb-oxides were always associated with clay minerals, and these clay minerals coated all soil particles including galena. Slag and/or clay minerals armored all Pb phases. The potential health hazard was reduced by the Pb mineralogy and soil chemistry present at the Cuba smelter site.

Acknowledgments

Table of Contents

Table of Contents

List of Figures

List of Tables

INTRODUCTION

This study investigated soils from the abandoned Cuba smelter site in Socorro, New Mexico and emphasized lead (Pb) availability and Pb concentration distribution in relation to possible health hazards. Important questions asked by this study include:

- Is Pb concentrated in a particular grain-size fraction?
- What are the chemical and physical conditions of the soil?
- How does an arid environment affect Pb mobility?
- What Pb minerals are present in the soil and are these minerals soluble under the present soil conditions?
- Is there a health threat when these factors are considered?

Lead contamination is a major concern because it poses a significant health threat particularly to children (Ewers and Schlipköter, 1991). Pb adversely affects the nervous and cardiovascular systems and the organs, especially the kidneys. Pb may even be carcinogenic based on animal studies (EPA, 1994). Pb poisoning remains the most common yet preventable health problem in young children in the United States (Grogin and Merians, 1997). Children with blood poisoning from Pb are at an increased risk for behavioral disturbances, decreased intelligence, and hematological (blood) disorders (Grogin and Merians, 1997). Children playing in contaminated soils or houses with Pb paint are at increased risk for Pb exposure. The health threat from Pb is accentuated when people inadvertently work or play in contaminated soils, air, dusts, or paints.

The determination of health threat in soil or groundwater is generally based upon contaminant concentration. For example, the U.S. Environmental Protection Agency (EPA) considers Pb contamination in residential soils a health threat whenever Pb levels exceed 500 parts per million (ppm), and as a result many "clean ups" or remedial actions

have been based on these guidelines alone. Unfortunately, these guidelines may not be representative of the actual health threat presented by a site. An arbitrary action level may not be appropriate for all sites, and any remedial actions based on these guidelines may not adequately address each site's unique physical and chemical conditions, such as Pb mineralogy, Pb concentration versus grain-size, and reactivity of Pb particles. For example, consider a site where health threats are minimized due to unique chemical and physical conditions, but Pb in soils is 1,500 ppm. Any "clean up" at this site would still be obligated by the EPA to reach a Pb level of 500 ppm. So, this hypothetical site may be considered a greater health threat than it actually poses and undergo costly and unnecessary remediation.

The Pb in soils guideline was revised when the EPA published new guidance with the Integrated Exposure Uptake Biokinetic model (IEUBK) in 1994. This model is used to evaluate the health risk of Pb in soils by evaluating the correlation of blood-Pb levels with soil-lead levels. The EPA, also, recommended site-specific assessment of Pb availability and distribution in soils especially at mining sites (Renner, 1995). Therefore, Pb concentration should not be the only consideration for cleanup, but used in conjunction with a thorough understanding of the soil's physical and chemical conditions and their relationship to Pb concentration and the overall health threat.

Health hazards associated with Pb contaminated soils are controlled by concentration, spatial distribution, and availability. The evaluation of these hazards is called risk assessment. The spatial or grain-size distribution of Pb-bearing particles should be determined during risk assessment, and it should ultimately be considered when designing a remediation strategy.

Determination of either whole-soil Pb or Pb concentration in a single grain-size fraction (e.g. Cepeda, 1987; Pace and Giulio, 1987; Schmitt and others, 1988; Sanders, 1990) may skew risk assessment and underestimate or overestimate the potential health

threat. For example, analysis of only the clay fraction and its Pb concentration may indicate hazardous concentrations, but the clay fraction may represent a small percentage of the total soil. So, risk evaluation based only on one soil fraction without the entire soil sample concentrations can skew risk assessment at a particular site.

Risk assessment should also include determining availability of Pb. Availability is a qualitative term relating to how accessible Pb may be to dissolution by soil solutions, gastrointestinal (GI) fluids or groundwater. Sandstead (1988) differentiates bioavailability from availability by indicating that bioavailability includes absorption and utilization by an organism. Only a fraction of the total Pb may contribute to the overall availability depending on how that Pb interacts with its environment (water, soil, air, or biosphere). Pb concentration alone is insufficient to determine health threat; other factors including the chemical form of Pb, soil pH, and soil texture will also influence bioavailability of Pb in soil (Chaney, 1988). These parameters will aid in defining the geochemical aspects of the soil, and how Pb will behave in a particular soil environment.

PREVIOUS WORK

Lead Contamination Studies in New Mexico

New Mexico has a long mining history; minerals have been exploited by Native Americans, the Spanish, and modern settlers for hundreds to thousands of years. Many mountains around the state host adits, mines, and tailings piles along their slopes.

Several sites around New Mexico have been evaluated for clean-up using various methods with some sites mainly relying on Pb concentration alone. Several mining areas in New Mexico of recent environmental interest include Socorro, Pecos, and Silver City (Figure 1).
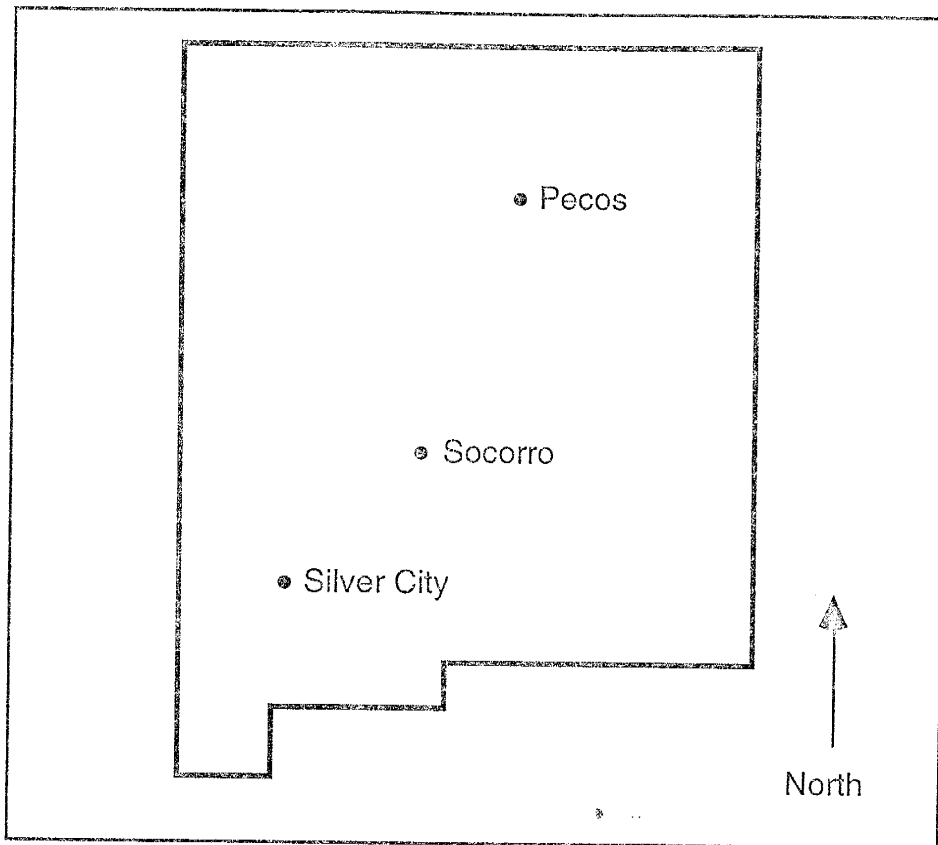
Figure 1: Map of the state of New Mexico showing the approximate locations of Socorro, Pecos, and Silver City where previous investigations concerning Pb contamination were undertaken.

Research of Lead Contamination at Smelter Sites Near Socorro, New Mexico

Socorro experienced a mining boom before the turn of the century. The mining wealth attracted many businessmen, and soon two smelters established themselves in the vicinity of Socorro. The smelters were the Cuba Smelter (investigated in this study) and the Billing Smelter. The Billing Smelter was the larger and more successful of the two. The Billing smelter site was remediated as an emergency action under the Comprehensive Environmental Response, Compensation and Liability Act (CERCLA) in 1990. The Cuba smelter site was also remediated as an emergency action under CERCLA, and the work was completed in 1994.

The chemical and physical nature of Billing smelter site soils was investigated by Austin and others (1993a and 1993b); they determined soil chemistry, Pb distribution, and Pb concentration versus depth. Soils were collected from near the main slag pile and another area downwind from the smelter exhaust. They noted that the greatest Pb concentration was in the finer grain-size fractions, especially in the clay fraction, and that these fine fractions comprised only a small portion of the total soil (clay-size was 1-3 % of soil mass). Austin and others (1993a) determined Pb contamination in undisturbed areas is limited to the first few inches of the soil horizon, and the lack of contamination at depth indicates the Pb is not downwardly mobile. They concluded that Pb was present in the Billing smelter site soils, but it is predominantly in the clay-size fraction and immobile in the alkaline soils.

Availability of metals to plants has been addressed for both smelter sites in Socorro. Brandvold and others (1996) analyzed soil and plant material from the Billing smelter site and the Cuba smelter site. Data for plants at the Billing smelter site was presented previously by Austin and others (1993b). Plants sampled included cacti, mesquite, creosote, fourwing saltbush, snakeweed, and dropseed grasses; both roots and foliage were collected. Soil was gathered from adjacent to the plant as well. Soils and plants were

analyzed for heavy metals including Pb. Overall, Brandvold and others (1996) noted that Pb in plants increased as Pb in soils increased. As the Pb increases in both materials, the uptake of Pb actually decreases as indicated by the biological absorption coefficient (BAC). The BAC is the ratio of Pb in the plant to Pb in the soil. For both sites the BAC decreased by 1 to 2 orders of magnitude as Pb increased in the soils. The only exceptions are the grasses and snakeweed which do not exhibit a 1 to 2 order of magnitude decrease in their BAC values. Considering this behavior, Brandvold and others (1996) concluded that some of the Pb must be unavailable, or the plants are capable of limiting their uptake.

Research of Lead Contamination Near Pecos, New Mexico

Several areas near Pecos, New Mexico have been under investigation to determine what impacts an abandoned Pb mill and mine had on the area. Three areas of primary concern are the Terei ɔ mine, the tailing piles associated with the El Molino mill in Alamitos canyon near the village of Pecos, and several U.S. Forest Service roads and campgrounds.

The Tererro mine primarily exploited a massive sulfide deposit for Zn and Pb, and they also extracted minor amounts of precious metals. The present concern arises over the waste rock pile. Johnson and Deeds (1995a) describe it as very heterogeneous but dominated by gangue minerals and pyrite (FeS_2) with some galena (PbS) and sphalerite (ZnS). The presence of pyrite may lead to acid mine drainage problems via seeps and springs along the base of the waste rock pile. These seeps and springs feed Willow Creek just upstream from its confluence with the Pecos River. Fortunately, the waste rock pile is in contact with Paleozoic limestone which has a strong acid neutralizing potential (ANP), so the potential exists for leachate buffering and metal attenuation by the native rocks. Analysis of the waste rock indicates that Pb, Zn, Cd, and Cu concentrations exceed regulatory levels in both whole samples and Toxicity Characteristic Leachate Procedure

(TCLP) samples (Johnson and Deeds, 1995a). This site is still under investigation as directed by the state of New Mexico.

The ores from the Tererro mine were brought to El Molino via an aerial tramway for milling and processing. El Molino discharged unwanted slurry into Alamitos Creek creating several tailings ponds. Alamitos Canyon is now undergoing remediation and groundwater monitoring (Johnson and Deeds, 1995b). Also under remediation are several U.S. Forest Service roads and campgrounds north of the Tererro mine. Apparently, waste rock material from Tererro was used in construction of access roads and campgrounds in the 1970's. The Forest Service became aware of these problems in the 1980's when devegetated plumes formed downgradient of eroded areas along the roads and near the campgrounds (Koch and Barkmann, 1995).

The pathways of concern in the Pecos area are surface water and groundwater. Considering surface water, Willow Creek runs through the Tererro mine into the Pecos River, and further downstream Alamitos Creek flows into the Pecos River. Alamitos Creek formerly ran through tailings piles created by El Molino, but it now flows in an armored diversion channel through stabilized tailings ponds before reaching the Pecos River. Sediments from the Pecos River were sampled upstream and downstream from the mine and the mill. McLemore and others (1995) investigated grain-size distribution and Pb concentration distribution. They noted that distribution by physical transport of Pb particles by the Pecos River maintains the highest concentration in the finest grain-size fraction (silt and clay). The fine grain-sizes are generally below 10% of the sample mass. Groundwater at the mine and mill sites is currently under routine monitoring.

Research of Lead Contamination Near Silver City, New Mexico

Silver City, New Mexico has numerous active and inactive mines. These mines have created numerous stockpiles and tailings piles which may lead to contamination of soils, groundwater, and surface water. Availability of metals within the Hanover and Bullfrog tailings were investigated by Baker (1993) to determine ion mobility and plant uptake of heavy metals. Distribution of Pb versus grain-size was not determined. The tailings were derived from Zn-Pb sulfide vein deposits with sphalerite and galena as major ore minerals.

Surface water and airborne pathways were evaluated by analyzing soils, tailings, plants and surface water for the possibility of the release of heavy metals. Groundwater lies at a depth of 200 feet and was not investigated. Results showed tailings with elevated concentrations of Pb, Zn, and Cu. Two tailings samples had Pb values greater than 500 ppm. The tailings show signs of surface alteration with white precipitates forming on the edges of the piles presumably from pyrite oxidation. Transport of metals apparently halts at these edges where oxidation occurs.

Concentrations of Pb, Zn and Cu in surface soils were elevated, but concentrations dropped below background levels at depths of 2-4 cm. The soils have an overall negative Net Acid Producing Potential (NAPP) which indicates alkaline soil solutions. Plant uptake of heavy metals was minimal. No adverse effects from the tailings on surface water were noted. Baker (1993) concluded that ion mobility was reduced, and dissolved transport of heavy metals away from the tailings is unlikely due to the alkaline nature of the soils and the arid climate of the southwest. Conclusions concerning the Hanover and Bullfrog tailings indicate a cap would be adequate to minimize surface infiltration and aeolian transport.

GEOCHEMISTRY OF LEAD AND SULFUR

Chemical and Physical Behavior of Lead and Sulfur in Soils

In order to understand the Pb and sulfur behavior in soils at the Cuba smelter site, the chemical and physical nature of Pb and sulfur must be reviewed. Considering Pb chemistry, Pb is a member of the chalcophile elements which include Cu, Cd, Fe, Pb, Mn, Hg, Ag, and Zn. Generally, the chalcophiles will form insoluble oxides and carbonates in the oxidized state and insoluble sulfides in reducing conditions. The sulfide forms are often sought after as exploitable ore. The ore is mined and processed, which leaves behind tailings ponds, stockpiles and slag heaps. Mining activities may elevate metal concentrations in surrounding soils. These activities expose the ore to a hostile environment where oxidizing fluids (oxygen and water attempting to scavenge electrons) attack the original minerals. Oxidizing reactions are generally exothermic and quick (hours to days). The ore minerals may dissolve, followed by adsorption of the dissolved species or precipitation of a new mineral phase stable in the soil environment. We may understand how the ore behaves through evaluation of various physical and chemical soil properties.

Oxidation-Reduction Reactions of Lead and Sulfur

Oxidation of sulfide ores is the most important chemical reaction when considering the environmental consequences of mining activities. We must understand how Pb and sulfur particles will behave chemically in the soils at the Cuba smelter site to predict health threats related to these soils. Oxidation-Reduction (REDOX) reactions between cations (metals) and anions (non-metals) involve electron-sharing between elements. The elements form bonds and share electrons between each element's outer orbital. Cations donate electrons to anions and form an ionic bond; this is the basic bond for most minerals. The electron donor is oxidized, and the electron acceptor is reduced. Each element wants to donate or accept electrons until a stable group of 8 electrons fills its outer shell (orbital); this

is the octet rule. The number of electrons which an element wants to donate or accept is considered its valence charge. For example, Pb always has a valence of +2 and is willing to share 2 electrons with sulfur. Sulfur has a valence of -2 when it forms a sulfide compound with Pb, but it has a valence of +6 when forming a sulfate (SO_4^{-2}) compound with Pb. Both PbS and $PbSO_4$ have a net valence of zero. Both compounds are stable and have satisfied the octet rule by sharing electrons.

Sulfur is the site for oxidation-reduction reactions in metal sulfides. Sulfide (S= -2) must oxidize to sulfate (S= +6) with a total change in valence charge of 8 electrons. Likewise, oxygen is reduced from +2 to zero, and 4 oxygens donate a total of 8 electrons to sulfur. To achieve the transfer of 8 electrons during transformation of sulfide to sulfate, sulfur must form several metastable compounds. These metastable compounds are generally short-lived and transform readily to a more stable phase. The intermediate ions and molecules fall into several groups including polysulfides (S_n^{2-}), polythiosulfates ($S_nO_3^{2-}$), polythionates ($S_nO_6^{2-}$), sulfites, (SO_3^{2-}), and sulfates (SO_4^{2-}) (Williamson and Rimstidt, 1992).

Soil Chemistry and Lead Behavior

The chemical nature of the soil environment must be understood to predict Pb behavior. For example, soils, especially alkaline soils, have a large capacity for the immobilization of Pb and other heavy metals (Zimdahl and Skogerboe, 1977). In soils, as pH increases from acidic to alkaline, the adsorption of heavy metals increases (Elliot and others, 1986; Fuller and Davis, 1987; Kooner, 1993; Schulthess and Huang, 1990). Inorganic and organic particles absorb Pb and other metals. Adsorption occurs between metal ions (which hydrolyze in water) and a soil's mineral surfaces (clay minerals, oxides or hydroxides) (Evans, 1989). Adsorption occurring between metals and clay minerals is an electrostatic cation exchange reaction where positively charged cations in solution are

attracted to the permanent negative charge of clay minerals (Evans, 1989). The cation-exchange capacity (CEC) measures this attraction in terms of milliequivalents of ions per 100 grams of clay or absorbing material. Smectite and vermiculite are clay minerals with the greatest CEC due to large internal and external surface areas. Covalent bonds are stronger than electrostatic bonds. Covalent bonds form between metals and oxides or hydroxides, including goethite ($FeOOH$) and gibbsite ($Al_2(OH)_6$), creating an inner-sphere complex. The inner-sphere complex forms between the metal and the negatively charged, deprotonated surfaces of Al, Mn, and Fe oxides or hydroxides. Besides inorganic adsorption, metals retention occurs with organic acids (humic and fulvic) creating inner sphere complexes (Evans, 1989).

Oxidation of Pyrite

Oxidation studies often focus on pyrite because it is the culprit for most acid rock drainage (ARD). Pyrite may be used as a proxy for discussing sulfide oxidation in a general sense. During pyrite oxidation the reaction demonstrates a first-order dependence on water. Therefore, the reaction rate is proportional to the amount of water present. The activation energy of the reaction indicates the reaction is not diffusion controlled, but it is chemically limited (Williamson and Rimstidt, 1994). The proposed model for pyrite oxidation and probably most chalcophile sulfides is electrochemical. An electrochemical reaction has distinct cathode and anode sites that electrons are transferred between. Williamson and Rimstidt (1994) suggest the oxidation reaction is an electrochemical reaction where electrons from the mineral are transferred to the aqueous oxidant via a discreet zone of solvent at the mineral surface.

Rimstidt and others (1994) describe sulfide oxidation by ferric iron (Fe^{3+}) and believe that iron plays a central role in the oxidation of sulfide minerals. The ferrous iron (Fe^{2+}) is often derived from the dissociation of pyrite during oxidation. Ferrous iron,

also, originates from iron-bearing oxides, carbonates, or silicates. At low pH values the reaction is slow, but rates may be dramatically increased by the activity of *Thiobacillus ferrooxidans* and related bacteria (Rimstidt and others, 1994). These bacteria derive metabolic energy by using oxygen to oxidize the ferrous iron to ferric iron. At neutral pH values ferric iron is rapidly oxidized to ferrous iron by dissolved oxygen in solution. Ferric iron is probably the primary oxidant of most sulfide minerals (Rimstidt and others, 1994). As more sulfide minerals are oxidized ferrous iron is produced and oxidizes to ferric iron, and the cycle continues. Excess ferric iron will eventually precipitate as iron oxyhydroxides.

Oxidation of Galena

Now that we have reviewed the general metal sulfide in terms of pyrite, lets consider galena, because it is the most common Pb phase at the Cuba smelter site. Galena will oxidize and form anglesite. For example, galena will oxidize in the presence of water and ferric iron under acidic conditions as indicated by the following reaction:

$$PbS + 8\ Fe^{3+} + 4\ H_2O \rightarrow 8\ H^+ + SO_4^{2-} + Pb^{2+} + 8\ Fe^{2+}$$
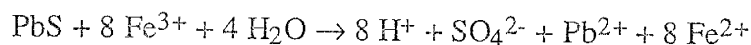
(Rimstidt and others, 1994). Originally, the iron is derived from pyrite dissolution or other ferrous iron-bearing minerals (oxides, silicates, or carbonates). The ferrous iron rapidly oxidizes to the ferric state in the presence of oxygen near a neutral pH. The broken water molecule releases 8 moles of H^+, lowering pH, and also releases oxygen which reacts with the sulfide forming sulfate. The SO_4^{2-} and Pb^{2+} will react and precipitate as anglesite.

$$Pb^{2+} + SO_4^{2-} \rightarrow PbSO_4$$
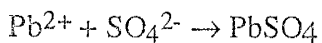
Rimstidt demonstrated that galena along with pyrite and arsenopyrite oxidize quickly. The general sequence of reaction rates is:

galena > arsenopyrite > pyrite > sphalerite > chalcopyrite

Of course, reaction rates for galena and arsenopyrite will be reduced over time by armoring effects of galena by anglesite and arsenopyrite by scorodite (hydrated iron arsenate, $FeAsO_4(H_2O)$). The reaction rate for these two minerals will eventually be controlled by diffusion of reactants through this armoring.

Rimstidt and others (1994) experimentally determined the rate law for galena at 25^oC near a pH of two. The reaction rate is dependent on surface area (A) and ferric iron concentration (m_{Fe}^{3+}).

Galena Rate Law: $r = -2.82 \times 10^{-3} (A) (m_{Fe}^{3+})^{0.98}$

Galena Activation Energy: $Ea = 40 \ KJ/mol = 9.56 \ kcal/mol$

The relatively large value (40 KJ/mol) for the activation energy suggests that the reaction rate is controlled by a chemical mechanism rather than diffusion through reaction products (Rimstidt and others, 1994). The greater the Ea the longer the reaction will take because more bonds are being broken and created.

To predict how minerals will behave in any environment we must understand the concepts of chemical equilibria and chemical kinetics. These concepts are used to predict the most stable phase of a system. The laws of thermodynamics are a method of describing the energy of a system at equilibrium, and how the system may behave. A balanced reaction at equilibrium is written as:

$$aA + bB \leftrightarrow cC + dD$$
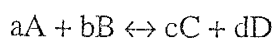
When a reaction achieves equilibrium the concentration of reactants and products maintain a constant ratio. This ratio is defined as the equilibrium constant (Keq).

$$K_{eq} = [C^c] [D^d] / [A^a] [B^b]$$

The Gibb's Free Energy (G) is a measure of a systems energy. For any reaction, ΔG is a measure of the driving force of the reaction. The free energy change, ΔG, of a reaction at standard state (T= 25° C, P = 1 atm.) is represented by the symbol: ΔG^o_R. The change in Gibb's Free Energy for a reaction is defined as:

$$\Delta G^o = \Delta H^o - \Delta S^o T$$

where ΔH^o is the enthalpy, ΔS^o is the entropy, and T is the temperature. Enthalpy is a measure of the heat liberated (exothermic) or adsorbed (endothermic) during the reaction. Entropy measures of the degree of disorder. Gibb's free energy is related to the equilibrium constant as follows:

$$\Delta G^o = -RT \ln K_{eq}$$

R is the gas constant (1.987 cal/degree*tmol), and T is temperature in degrees Kelvin.

The change in Gibbs Free Energy for any reaction, ΔG°_R, is calculated as follows:

$$\Delta G^\circ_R = \Sigma n_i \, G^\circ_F \text{ (products) } - \Sigma n_i \, G^\circ_F \text{ (reactants)}$$

where n_i is the molar coefficient in the balanced reaction and G°_F is the Gibb's Energy of Formation. When ΔG°_R is negative the reaction will occur in the forward direction, and a positive value indicates a backwards reaction.

If we consider the change in Gibb's free energy for the oxidation of galena by ferric iron:

$$PbS + 8\ Fe^{3+} + 4\ H_2O \rightarrow 8\ H^+ + SO_4^{2-} + Pb^{2+} + 8\ Fe^{2+}$$

By using data tabulated in Faure (1991) the ΔG°_R would be:

$\Delta G^\circ_R = [1(-177.75)+1(-5.85)+8(-18.85)] - [1(-22.9)+8(-1.12)+4(-56.687)]$

$\Delta G^\circ_R = [-334.4] - [258.6] = -75.8 \text{ (kcal/mol)}$

The change in free energy is negative, and the reaction goes forward. So the forward reaction proceeds favoring PbS oxidation producing SO_4^{2-} and Pb^{2+}, which is favored to form anglesite ($PbSO_4$).

$$SO_4^{2-} + Pb^{2+} \rightarrow PbSO_4$$
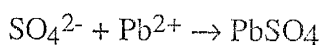
For anglesite formation the ΔG°_R would be:

$\Delta G^\circ_R = [-194.42] - [-5.85 + -177.75]$

$\Delta G^\circ_R = -10.82 \text{ (kcal/mol)}$

Anglesite would form after galena oxidation by ferric iron and water. Anglesite only forms in oxidizing conditions. This is important because the soils at the Cuba smelter site are an oxidizing environment, and we should expect oxidation products to form in these soils.

Physical Properties Related to Lead and Sulfur Behavior

The physical properties of a soil will affect Pb and sulfur behavior because the soil environment is where chemical reactions occur. One of the most important soil parameters is moisture content because all redox reactions are dependent upon water and the dissociation of water for the reactions to occur. Soil moisture is a reflection of the local climate (arid versus temperate) and precipitation rates. For example, precipitation in Socorro occurs as monsoons, which are short lived thunderstorms that cause high amounts of runoff with minimal infiltration of water into soils. Whereas slow gentle rains allow water to soak into a soil. Porosity and permeability are parameters used to describe soil pore space and how fluids move through soils. If a soil is well-drained leaving only residual amounts of water and mostly air in the pore spaces, porosity and permeability are high.

The micromorphology (relationship of soil particles to one another) of the soil is important as well. The inter-connectedness of pores and cementation affects water movement between soil particles. If the Pb is contained within a soil's cement or soil ped (agglomeration of soil particles), water and air may be limited by diffusion processes to reach the Pb grain. The size of the soil peds and individual particles will determine the reactivity because of the inverse relationship of surface area to size: as particle-size decreases, the surface area ratio increases. A clay-size particle will be more reactive than a sand sized particle because it has a greater surface area compared to the sand-size particle.

AVAILABILITY OF LEAD

Availability is a qualitative term used to describe what fraction of Pb in a system will react with liquids such as soil solutions, gastrointestinal (GI) fluids, or groundwater. Bioavailability is a measure of absorption and utilization of Pb by an organism. Availability decreases when conditions in a system prevent Pb from reacting or dissolving. Four factors control Pb availability:

- Pb mineralogy
- Soil chemistry
- Degree and nature of encapsulation of Pb particles
- Rate of Pb dissolution in the GI tract

Lead Mineralogy

Mineralogy controls Pb availability as shown by Davis and others (1992, 1993), Freeman and others (1992), and Ruby and others (1992, 1994). Pb mineralogy is a critical factor in determining availability because each Pb mineral or compound has characteristics which determine reactivity (Gunn and others, 1988). For example, oxidation of ore material (e.g. galena (PbS) altering to anglesite ($PbSO_4$)) can reduce availability by the creation of a mineralized rim with a lower solubility ($PbSO_4$) surrounding the more soluble grain (PbS). When a grain is encapsulated by a mineral of lower solubility the grain is considered armored. The armoring limits reactive material, water and oxygen, from reaching the galena. The oxidation reactions slow and become limited by diffusion of oxidants through the anglesite to the galena. As the oxidizing potential (Eh) increases PbS is expected to become armored by $PbSO_4$ (Garrels and Christ, 1966).

Soil Chemistry and Lead Behavior

Soil chemistry is discussed in detail in the Soil Chemistry And Lead Behavior section.

Encapsulation of Lead Particles

Encapsulation reduces availability by creating a barrier between the encapsulated particle and pore waters. Clay minerals in the soil, gangue minerals associated with Pb in the original ore material, or glass from the smelter process may encapsulate Pb-particles. The precipitation and/or absorption of other mineral phases upon a more soluble grain will reduce surface area available for dissolution (Sposito, 1989; Evans, 1993; Kargbo, 1994). For example, quartz, jarosite, or iron-oxides (Fe-oxides) may precipitate from a soil solution onto a PbS surface and effectively armor the PbS from the soil solution. Clay mineral coatings also reduce availability by limiting available surface area (Davis and others, 1993).

Lead Behavior in the Gastrointestinal Tract

Dissolution kinetics of mine waste under gastrointestinal (GI) tract conditions has been the focus of several recent availability studies (Davis and others, 1992; Ruby and others, 1992). Laboratory studies conducted with Butte, Montana soils successfully showed that anglesite coating of PbS lowers Pb bioavailability (Davis and others, 1992). These studies used contaminated soils which contained galena with anglesite armoring and jarosite precipitates. Rabbits were fed contaminated soils under laboratory conditions. A pure Pb compound and Pb acetate were also fed to the rabbits. The mine waste was the most resistant to GI fluids and dissolution during GI tract residence time. Only 6% of the total Pb content of galena was absorbed through the rabbits' small intestine which was 5 times less than the absorption rate of the pure Pb and Pb acetate in the rabbits. The

armored galena had a lower bioavailability that the pure Pb and Pb acetate. The decrease in bioavailability was attributed to the geochemical factors controlling availability: mineralogy, encapsulation, rinding or armoring, and particle size.

Another similar study used rats as the test population (Freeman and others, 1992). Once again Butte, Montana soils were fed to a control group to determine relative bioavailability. Freeman and others (1992) calculated a relative bioavailability based on Pb levels in blood, tissue, and bone. The greatest bioavailability was 20% in blood, 9% in bone, and 8% in liver analyses. These values were considered low when compared to studies of rats fed soils contaminated with Pb paint, Pb from auto exhaust, or Pb-acetate which had bioavailabilities of 70% to 80%. Once again the mining waste had a much lower bioavailability.

One important outcome of these bioavailability studies is the result of comparing mine waste to other Pb compounds. Pb compounds were originally used to determine Pb dissolution rates and subsequent clean up levels.

Ruby and others (1992), also, investigated kinetic limitations of Pb particles during residence time in the GI tract. An acid bath of hydrochloric acid was used to test Pb solubility from pure $PbSO_4$ and mine-waste soil under GI tract type conditions. GI tract conditions were simulated using a solution with a pH=1.8 and maintaining a residence time of 2 hours. The mine soil had a lower dissolution rate than the pure $PbSO_4$. They determined dissolution kinetics of Pb-bearing minerals must be considered when evaluating Pb-availability, especially when secondary phases have encapsulated the primary Pb-phase.

Pb availability in soils is controlled by the mineralogy of Pb. Both the composition of the original ore and secondary products which formed in the soil. The mineralogy determines how Pb behaves in the soil environment and GI tract. Therefore, Pb mineralogy must be determined to evaluate availability.

Smelter Processes

The processes of Pb smelting will help explain the particles and slag textures found in soils at the Cuba smelter site. A smelter and stamp mill were located at this site. The smelter uses high temperatures to melt crushed ore and separate Pb from other elements in the ore. The stamp mill uses Hg amalgamation processes to remove Pb from the crushed ore to create Pb bullion.

Three major steps are involved in processing PbS ore (Henry and Heinke, 1989):

- Sintering
- Reduction
- Refining

Before processing, the PbS ore is broken up and concentrated by crushing. During sintering the PbS is heated and oxidized to produce PbO sinter particles and sulfur dioxide (SO_2) gas. Sinters are silt-sized ranging from 5 to 40 μ. Equal amounts of the S partition into SO_2 gas and slag. In the reduction process, oxygen is removed from PbO in a blast furnace to form molten Pb bullion. Further purification occurs during refining, and many elements including antimony, arsenic, bismuth, tin, zinc, precious and other metals are removed. These metals are partitioned into dross. The end result is very pure Pb ingots or pigs with close to 99.99% pure Pb (Henry and Heinke, 1989).

The by-products of smelting are dusts, slag, and dross particles. During the sintering and reduction stages approximately 500 pounds of particles per ton of processed ore are released from modern lead smelters (Henry and Heinke, 1989). Immiscible slag and dross form on the melt surface as separate phases from the metallic matte. Both float to the surface of the metallic matte because they have a lower density than the molten Pb and metals. Slag vitrifies as a silicate and becomes a receptacle for gangue minerals and

unreduced oxides which did not react during the reduction step (Coudurier and others, 1985). Dross forms a metallic sulfide surface on the molten Pb during removal of the metallic impurities. The dross will solidify as a mixture of metal sulfides and alloys, and drops are often entrained in the slag. The composition of slag and dross will be highly varied and dependent on the original ore composition.

Particles from a modern Pb smelter have been characterized using electron microprobe analysis and reflected light microscopy. One study examined dust particles (silt-sized and less) that were collected in the active Herculaneum Lead Smelter located in Herculaneum, Missouri (Karakus and Hagni, 1991). These samples originated from the blast furnace, the sinter plant scrubber, the sinter plant crusher, the dross furnace, and the refinery. Many phases were identified throughout the smelter including (Karakus and Hagni, 1991) :

- galena fragments

- unreacted original feed: pyrite, chalcopyrite, and sphalerite

- slag

- dross phases: melted PbS, metallic Pb and Cu, metal alloys (mixtures of Cu, Ni, Zn, Ag, and Sb), and sulfides (Ni-sulfide, Cu-sulfide, and Cu-Pb-Sulfide)

- coke fragments (fluxstone)

- oxidized particles: bornite, chalcocite, covellite, magnetite, hematite, and goethite

Examination showed that dust samples from each location contained galena, pyrite, and chalcopyrite. These unreacted sulfides were easily identified by their angular shapes and fragmental nature, preservation of gangue, and sulfide relationships, especially when compared to rounded metal sulfide phases (dross) and slag. The dross and slag are the result of processing. The unreacted particles contained few impurities whereas reacted

particles displayed intermediate solid solution and exsolution between sulfides and oxides. Metal sulfides occurred as large free particles or enclosed in sulfide dross particles.

Karakus and Hagni (1991) also noted slag and dross particles with interesting textures in the modern smelter dusts. They characterized the slag as having Pb disseminated throughout a vitreous matrix. The slag was a mixture of calcium silicate and zinc iron oxide. Eutectic textures were common in the dross, and the eutectic composition texture was a mixture of galena and copper sulfide (Cu_2S).

CUBA SMELTER SITE DESCRIPTION AND HISTORY

As previously noted, Socorro, New Mexico experienced a mining boom from 1880-1900. Silver, zinc, and lead ores were brought from the Magdalena and Socorro mining districts to the community of Socorro for smelting (Fig 2). Two smelters were located near Socorro: the Billing Smelter and the Cuba Smelter. The Cuba smelter site is the focus of this study.

Eveleth (1983) describes the history of the abandoned Cuba smelter site. The industrial site was active from 1881 until the beginning of World War I (WWI). Two precious and base metal recovery operations existed at the site: a crushing plant or stamp mill and the smelter. The original smelter, known as the New Orleans and La Jolla, opened in 1881, but it closed shortly thereafter. The smelter reopened as the Graphic Smelter in 1895 and operated until the turn of the century. The Cuba Brick Plant operated at the site from 1900 until 1905. Finally, the Cuba Smelter reopened again in 1905, but apparently it shut down again by WWI. The Torrance Stamp Mill only operated from 1882-1884.

The abandoned Cuba smelter site is located in the Rio Grande rift valley. The climate is arid with less than 25 cm of precipitation per year. The smelter site lies on flood plain, low terrace, and alluvial fan deposits of the ancestral Rio Grande valley (Osburn, 1984). The site covers about three acres between Interstate 25 and a small residential neighborhood on the southeast side of the city of Socorro (Fig 3). The smelter and stamp mill were built on and along the slope of a natural terrace, presumably to take advantage of gravity during operation (Figs 4 and 5). The smelter structures and equipment have been gone for many years (Fig 6).
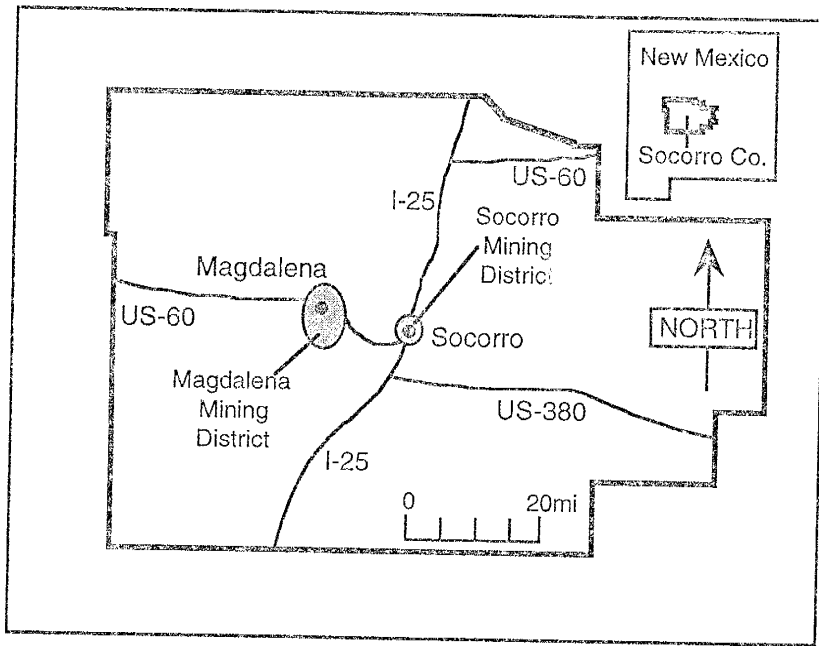
Figure 2: Map of Socorro County, New Mexico, showing the city of Socorro and the Socorro and Magdalena mining districts.
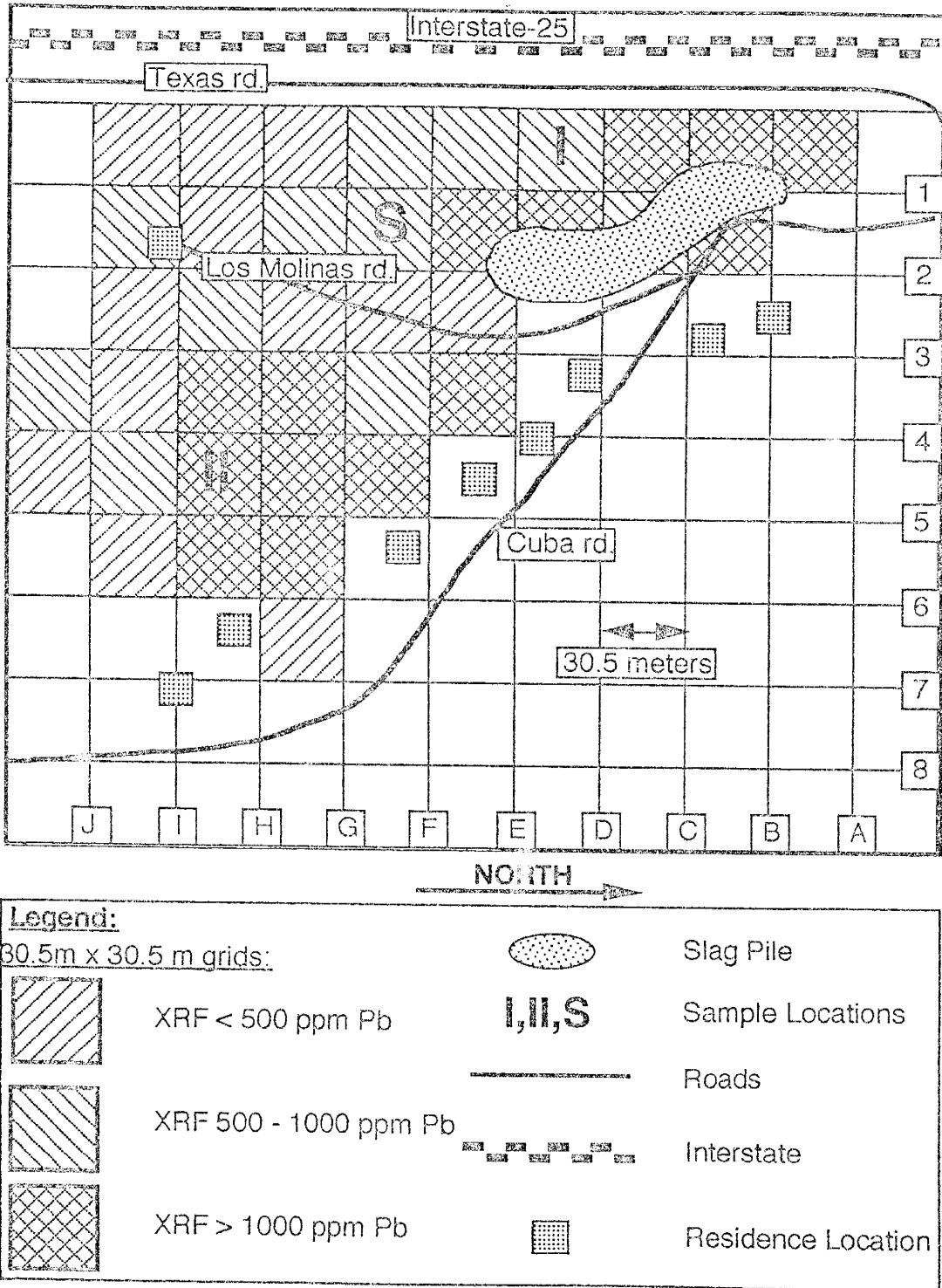
Figure 3: Map of the Cuba Smelter site, Socorro New Mexico showing Pb distribution in soils determined by x-ray fluoresence by EPA contractors.
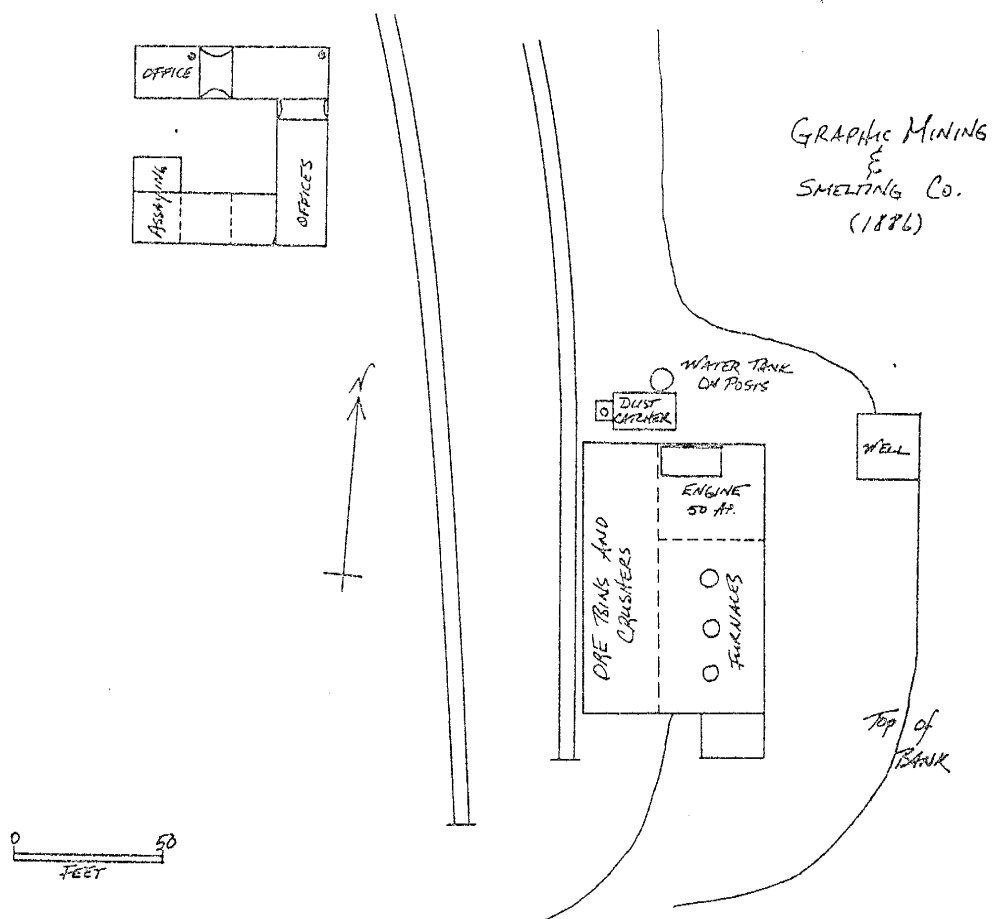
Figure 4: Sanborne Insurance Map of the Graphic Mining and Smelting Company circa 1886. Several important aspects of the smelter are represented including the three furnaces, ore bins and crushers, and the dust catcher. The map shows the smelter is located above the "top of bank". An assay laboratory was also onsite in the office facility. The map is reproduced from Nieman (1972).

Figure 5: Historical photo of the Cuba Smelter site taken in 1893. The Graphic Smelter, as it was called in 1893, is in the foreground with the Torrance Stamp Mill in the background. The smelter complex is built onto the hillside or terrace to use gravity feed during production. This view is to the southwest. The photo was taken by Socorro photographer, Joseph Edward Smith (Mckee and Wilson, 1974).
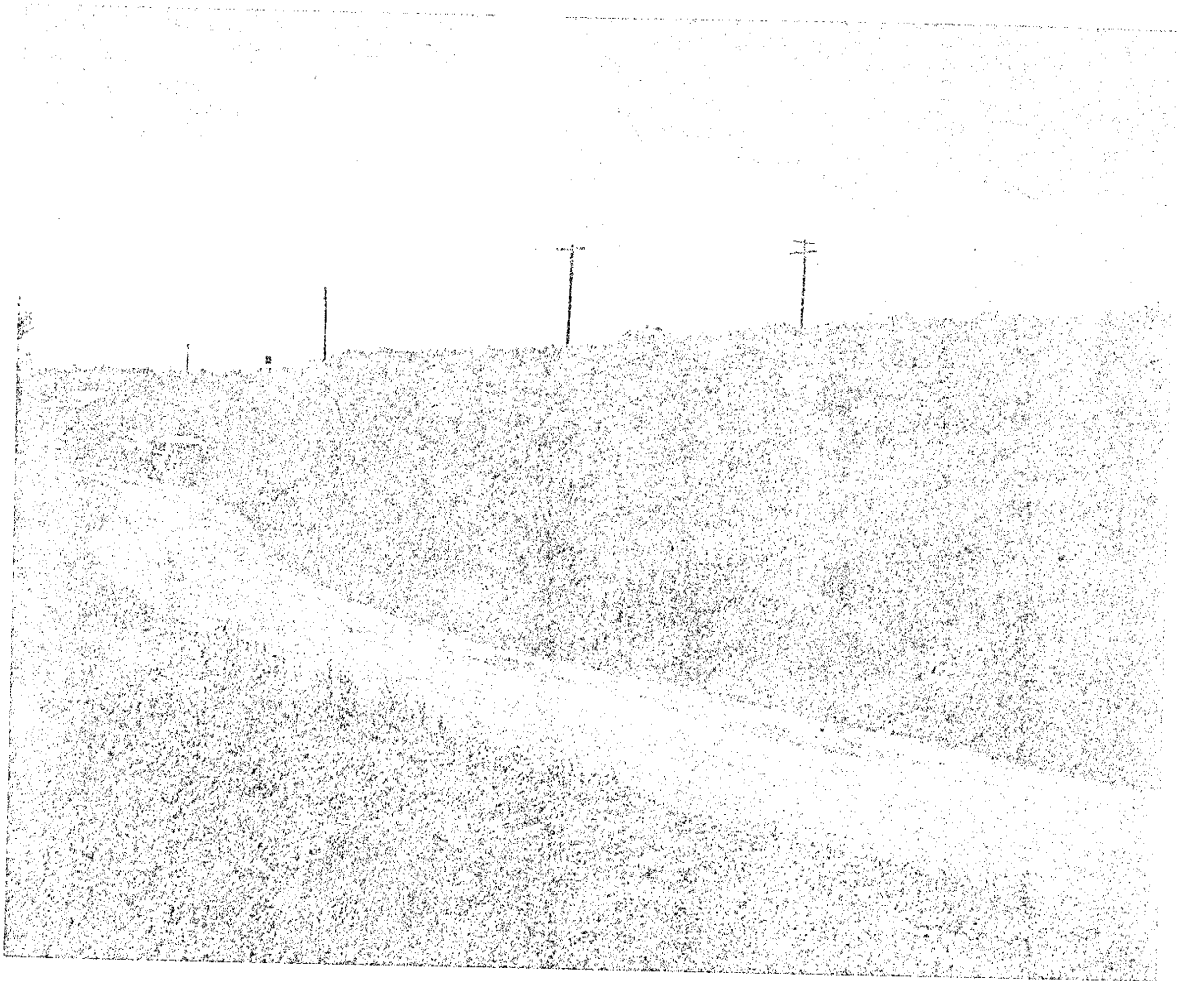
Figure 6: The Cuba Smelter site prior to remediation in 1993. The vantage point has the same perspective as the historical photo (Figure 5). The smelter was located on the terrace in the center of this photo. The Torrance Stamp Mill was built on the hillside above the volkswagen parked on Los Molinas road. The vegetation appears to be flourishing at the site.

PREVIOUS INVESTIGATIONS AT THE CUBA SMELTER SITE

In 1990, the state of New Mexico investigated the Cuba smelter site and produced a Screening Site Investigation (SSI). The preliminary assessment of the SSI was that soils at the site had elevated concentrations of heavy metals including Pb and Hg. In fact, contamination was so widespread that Socorro residents, who were interviewed by the state, indicated mercury could be collected at the site by digging small pits near the smelter and stamp mill foundations (it would puddle in the bottom of the pits!).

Sanders (1990) indicated that four pathways existed for the release of hazardous material from the Cuba smelter site. The pathways for possible release were determined to be:

- Airborne

- Surface water

- Ground water

- Onsite/direct contact

The pathways were evaluated by the state through soil, slag, and water sampling. A background level for Pb in soils was established by taking a soil sample 1,650 feet southwest of the site; background soil Pb concentration is 48 ppm. Soil transects to the north and south were sampled to determine the areal extent of contaminants. Elevated Pb concentrations were detected to 1,025 feet south of the site and 75 feet north of the site. The northern transect was probably not representative of conditions due to disturbed areas where roads and houses have been built. Surface water was not present in the irrigation ditch running through the site during the SSI, but soil samples were collected in the ditch and revealed 140 ppm Pb near the slag pile and 31 ppm Pb near the stamp mill. Sanders (1990) believed that these Pb levels would not "negatively impact the quality of water that

flows in the ditch during the irrigation season." Sanders (1990) also noted that the site lies within a 500-year floodplain which is important when considering physical transport of particles offsite.

The state of New Mexico collected groundwater samples from several private irrigation wells and an onsite EPA well placed near the southeastern side of the slag pile. All irrigation wells had no evidence of contamination, whereas the EPA well did show evidence of contamination. The samples analyzed from the EPA well were both unfiltered and filtered. The unfiltered sample contained Pb levels of 0.98 milligrams/liter (mg/L), and the filtered sample contained Pb levels below the detection limit of 0.005 mg/L. The New Mexico Water Quality Control Commission standards for Pb are 0.05 mg/L, so the unfiltered sample exceeded drinking water standards.

Soils and slag were sampled and showed elevated heavy metal concentrations. Soil Pb values ranged from 200 ppm to 37,400 ppm which are all elevated relative to the background sample. Two slag samples were analyzed for both total and leachable metals. Total metals showed elevated Cu, Zn, As, Hg, and Pb; Pb levels were 20,700 ppm and 25,800 ppm for the two samples. When Toxicity Characteristic Leachate Procedure (TCLP) leachate was tested, all metals were below the Resource Conservation Restoration Act (RCRA) toxicity limits. Considering these results Sanders (1990) concluded "that the high amounts of heavy metals contained in the 11,000 m³ of slag on site are not readily leached from the siliceous matrix, and may therefore be relatively immobile."

New Mexico decided a more in-depth investigation was warranted. Subsequently, contractors for the EPA conducted an X-ray fluorescence (XRF) survey to determine total Pb content of the soils. A grid system was surveyed consisting of 30.5 m by 30.5 m squares. Within each square, thirteen evenly distributed sample sites (Fig. 4) were measured with a portable XRF unit, and the 13 values were averaged to determine a value for each grid. Confirmation samples were analyzed at an off-site laboratory to ensure XRF

accuracy in the field. Soils at the site were found to exceed the EPA's "action level" of 500-1,000 ppm Pb.

The site was slated for emergency clean up under CERCLA with a $1.5 million budget. During remediation approximately 25,000 cubic yards of material were removed; two to three feet of material was removed from the terrace, and one foot was removed from the agricultural field (B. Ridpath, pers. comm. 1994). A cap composed of native material from south of the site was placed over the areas which previously had the greatest contamination, and a chain link fence was erected around the site (B. Ridpath, pers. comm. 1994). Remediation concluded in January 1994.
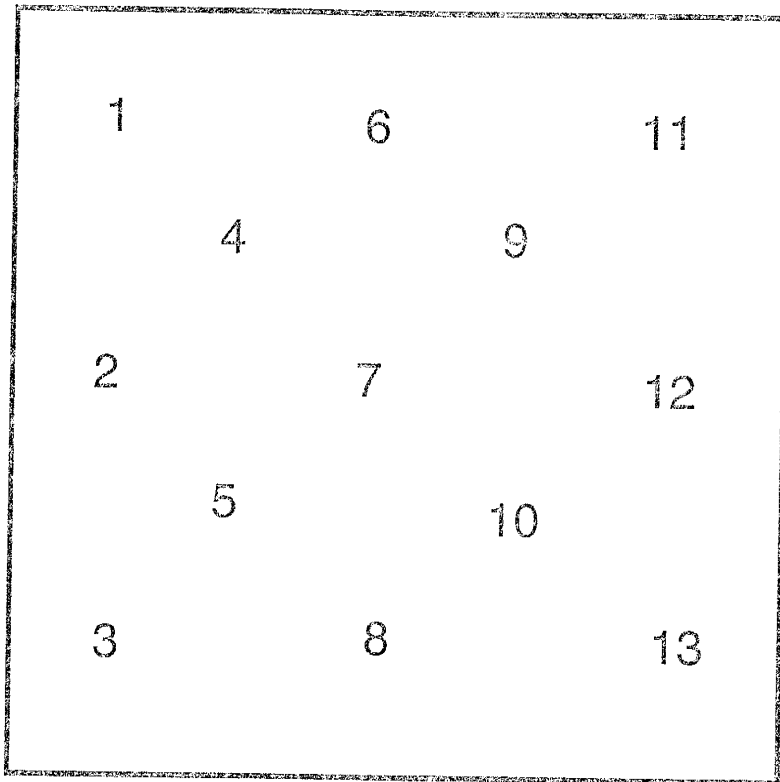
Figure 7: Sample locations and distribution within the 30.5 meter by 30.5 meter squares for the XRF survey and CS I and CS II (This study). Sample location #1 is located in the southwest corner.

SAMPLING AND ANALYTICAL TECHNIQUES

This study investigated soil samples from the Cuba smelter site to determine textural and chemical characteristics. The following sections describe sample locations, test methods, and analyses.

Soil Sampling Methods

Soils from the Cuba Smelter site were collected in early 1993 prior to the site's remediation. The sampling distribution for this study is based on the grid system used in the EPA contractor's XRF study. As shown in Figure 4, thirteen evenly distributed soil samples throughout the 30.5 m by 30.5 m (100' by 100') squares were taken. Samples within the 30.5 m by 30.5 m squares are denoted with Arabic numerals (1-13). Sample 1 is approximately 3 m from the southwest corner of the square and sample 13 is about 3 m from the northeast corner of the square. Two grids were sampled because they had high soil Pb concentrations as reported in the XRF study. The location of grid CS I (Cuba Smelter, Sample Grid #1) lies near the smelter foundation on top of the terrace with a reported Pb concentration of 791 ppm (EPA, 1993) (Fig 2). Grid CS II (Cuba Smelter, Sample Grid #2), in a fallow agricultural field essentially at the base of the stamp mill, had a reported Pb concentration of 1,650 ppm Pb (EPA 1993); (Fig 3). Several slag nodules from the soil surface were collected near the smelter foundation to ascertain Pb availability as well (Fig 3).

Two types of samples were collected for each grid: thirteen "grab" samples of the upper three inches of loose surficial material, and intact soil samples that were impregnated with epoxy to maintain soil microstructures. After removing the >2 mm fraction, the "grab" samples were used for soil chemistry, X-ray diffraction (XRD), and particle-size analyses. The intact samples were encased *in situ* using aerosol foam insulation, which is analogous to using a plaster jacket. Small trenches approximately nine inches deep were

dug around the samples, the foam was sprayed onto the soil surface and into the trenches to support the sides of the sample and allowed to dry overnight. The samples were carefully removed with a shovel, turned upside down, and the bottom was covered with foam to completely encase the samples before transportation to the lab. The intact samples are located between "grab" samples 1 and 2 for both grids. The intact samples were impregnated with epoxy containing a blue stain, cut, and mounted as thin-sections, which were used for petrographic and microprobe analyses. Several small trenches were dug to study soil textures at the field scale and to collect soil samples for contamination versus depth studies.

Grain-Size Methods and Analysis

The "grab" samples were passed through a 2mm sieve to remove gravel and large organic material. The < 2mm fraction was separated into sand, silt/clay, and clay sizes. First, a wet sieve shaker with a #200 mesh sieve was used to separate sand-size particles from the silt and clay. Sedimentation techniques based on Stoke's Law were used to isolate the clay-size fraction. Sand and clay masses were based on the separated portions. Silt values were calculated by subtracting sand and clay values from the starting mass of the <2mm sample according to standard New Mexico Bureau of Mines and Mineral Resources Clay Lab techniques. Silt percentage was calculated based on sand and clay values as follows:

$$Silt\ (\%) = 100\% - (Sand\ (\%) + Clay\ (\%))$$

X-Ray Diffraction Methods and Analysis

X-ray Diffraction (XRD) was performed on oriented clay (<2 μ) slides and random powder mounts. Oriented clay slides were made by taking a small soil sample (20-25

grams) of the <2mm fraction and dispersing it in 100 mL of distilled water, waiting 5 minutes and decanting the supernatant. This was the clay-size fraction or <2 μ equivalent spherical diameter (<2 μ e.s.d.) in size (Moore and Reynolds, 1989). The oriented slides were analyzed on a Rigaku diffractometer from 2-35°2Θ, 2°2Θ per minute with Cu-radiation. Three types of XRD analyses were selected: air-dried, glycolated, and heated.

Random powder mounts were prepared from soil samples of the <2 mm size fraction. Approximately 1 gram of sample was ground to pass a #70 mesh sieve. The crushed samples were loaded into an aluminum holder and placed directly onto a Norelco diffractometer and run from 2-55°2Θ, 2°2Θ per minute with Cu-radiation.

Electron Microprobe Methods and Analysis

Electron microprobe analysis was used to determine the spatial and mineralogical distribution of Pb in the samples. Data collection was performed on a JEOL 733 superprobe with Oxford link eXl II at the University of New Mexico. Electron microprobe analysis produced back-scattered electron (BSE) images that distinguish variations in composition because the back-scattered electron intensity is proportional to a phase's atomic weight. X-ray elemental mapping was also performed on the microprobe. Wavelength dispersive (WDS) and energy dispersive (EDS) analyses were used to collect qualitative data on the chemical composition of phases on a microscopic scale. WDS replaced EDS when Pb and S are in the same sample because the EDS' Pb and S peaks interfere with one another. The WDS and EDS mapping was used in conjunction with video imaging to create element maps. The element map intensity is proportional to element concentration. For example, areas of high Pb concentration show up as white on element maps. EDS X-ray spectra provide qualitative compositional data for all elements present in the thin-section in the area under the electron beam.

Electron microprobe analysis has been used effectively to study Pb-contaminated soils in Montana and Colorado (Link and others, 1994; Davis and others, 1992; Ruby and others, 1992; Davis and others, 1993). In addition, soils near a copper smelter in Poland were investigated by electron microprobe analysis by Kowalinski and Weber in 1990 to identify heavy metal mineralogy.

Soil Chemistry Methods and Analysis

Soil chemical analyses on Cuba smelter site soils included the determination of Pb concentration in bulk, sand, and clay samples, bulk sample pH, and Net Acid Production Potential (NAPP) of bulk samples.

Pb concentration of powdered samples was determined using acid digestion and atomic absorption (AA). The samples were microwave digested in nitric acid. Analyses were done on bulk soil samples of the <2 mm fraction, on the sand (<2mm-63µ), and on clay (<2µ e.s.d.) grain-size fractions. Silt Pb-values were calculated, based on the following equation:

$$\text{Silt } Pb_{(ppm)} = \text{Bulk } Pb_{(ppm)} - [(\%Sand * Sand\ Pb_{(ppm)}) + (\%Clay * Clay\ Pb_{(ppm)})]$$

Soil pH was determined with a pH electrode. A soil suspension was produced by mixing a bulk soil sample with distilled water in a 1:2 ratio. The aliquot was allowed to settle before measurement. The pH of the supernatant liquid was then measured and recorded.

Net Acid Producing Potential (NAPP) determination follows EPA method protocol for mine waste soils (Smith and others, 1974). This method is used for predicting acid

rock drainage (ARD) related to mining activities. NAPP is based upon the difference between the APP and ANP:

$$NAPP = APP - ANP$$

where APP is acid producing potential, and ANP is acid neutralizing potential. The APP determination is based on a titration of the acid produced by the oxidation of reduced sulfur in the sample. The ANP is determined by neutralizing the carbonates in the soil with an excess of standardized hydrochloric acid and a back titration to determine the amount of excess acid. The NAPP is then determined by calculation.

A positive value of NAPP indicates that the generation of acid will consume all neutralizing potential in the soil and continue to generate acidity. Whereas a negative value of NAPP indicates the soil will neutralize any acid generated within the soil. NAPP is reported in tons of $CaCO_3$ needed to neutralize 100 tons of the sample.

Evaluation of Analytical Uncertainty

Soil standards with a documented Pb concentration were submitted to evaluate analytical uncertainty. Two Montana soils were chosen because their Pb concentrations correspond to the Pb levels at the Cuba smelter site. The Montana soils chosen were SRM 2710 and SRM 2711 with Pb values of 5,532 ± 80 and 1,162 ± 31, respectively (NIST 1992a, NIST 1992b). At the 95 percent confidence level, the Pb concentration analysis, acid digestion followed by atomic absorption (AA), have a 2σ uncertainty of 12% - 32% (Table 1).

Uncertainty is related to these soil samples because they have a very heterogeneous distribution of Pb, and this Pb is present in relatively high concentrations. The AA is basically a tool for trace metal analysis and precision is lowered when sample dilutions are

necessary prior to analysis. Uncertainty probably also arises from incomplete digestion of the Pb phases in the soil. The AA analyses are routinely duplicated and the Cuba smelter site samples' duplicate runs have an excellent correlation of $r^2 = .99$ (Fig 5). Less soluble Pb-phases and soil heterogeneities cause uncertainty to increase in the Cuba smelter site soils.

Several calculated silt values were negative, probably a result of soil heterogeneity. This heterogeneity may have been inadvertently emphasized during sample preparation. Bulk samples were passed through a 2mm-mesh sieve and split into two subsamples. One was analyzed for Pb-concentration. Grain-size analyses were performed on the other subsample, then sand and clay fractions were examined for Pb values. The silt values were then calculated.

The negative silt values may also be explained by the "nugget effect", which occurs when a mineral is concentrated in "nuggets" and is not disseminated throughout the soil. The nuggets probably occur infrequently, but they have elevated concentrations of Pb compared to the other soil particles. For example, if a bulk sample contained fewer Pb-bearing "nuggets" than the grain-size sample, the silt calculation would come out with a low Pb concentration. The error is compounded by the bulk Pb being low and the sand and clay Pb concentrations being high. So, the calculation would report a low or negative silt-Pb value. Analytical uncertainty due to incomplete digestion of Pb may further compound the problem.

TABLE 1: Uncertainty For Pb Concentration Analysis

Montana Soil	Certified Pb Conc.(ppm)	Reported Pb Conc.(ppm)	Mean (ppm)	Uncertainty 1σ (ppm)	Uncertainty 2σ (ppm)
SRM 2710	5532± 80(1.4%)	5100	5500	5500 ± 872(16%)	5500 ± 1744(32%)
(NIST 1992a)		6500			
		4900			
SRM 2711	1162 ± 31(2.7 %)	1100	1070	1070 ± 60(6%)	1070 ± 120(12%)
(NIST 1992b)		1100			
		1000			
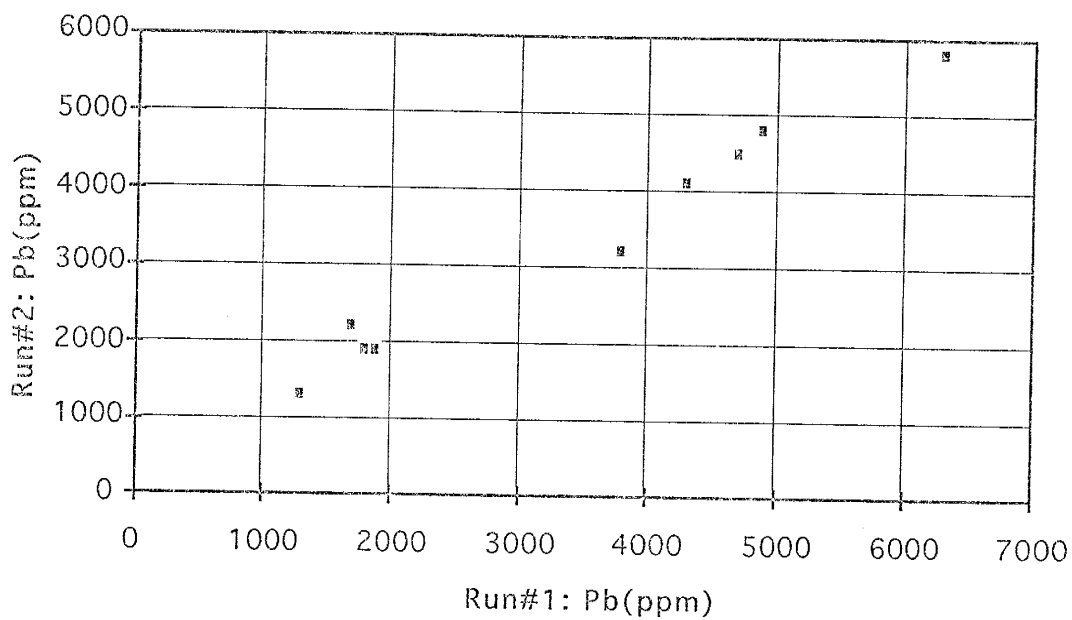
Figure 8: Plot showing correlation between duplicate runs of an AA sample. n=9, $r^2 = .99$.

RESULTS

Soil Chemical Analysis

Soil samples from the Cuba smelter site were analyzed for pH and NAPP. Soil chemical and textural data is presented in Table 2. Soil pH for all grid CS I and CS II samples is mildly alkaline ranging from pH=7.2 to 7.9 (Fig 9). The soils have negative values for Net Acid Producing Potential (NAPP) indicating any acid generated within the soils will be consumed by the neutralization potential of the soils (Fig 10). The NAPP ranges from -6.1 to -12.3 % $CaCO_3$ for terrace samples and from -1.7 to -10.6 for field samples. Most of the terrace samples had APP values below the detection limit of 0.3 % $CaCO_3$ with a maximum of 2.7 %$CaCO_3$. All of the field samples had detectable APP ranging from 1.3 to 7.8 %$CaCO_3$. All samples exhibited acid neutralization potential. The ANP for the terrace samples was 6.1 to 12.3 %$CaCO_3$, and ANP for field samples was 9.3 to 11.9 %$CaCO_3$.

Table 2: Chemical And Textural Analyses For Soils From The Cuba Smelter Site

| Sample ID	Bulk Soil					Particle-Size Distribution					
	Pb (ppm)	pH	APP	ANP (%CaCO3)	NAPP	Sand %	Pb (ppm)	Silt %	Pb (ppm)	Clay %	Pb (ppm)
CS I-1	1500	7.4	<0.03	12.3	-12.3	63	3300	30	-680	7	1500
CS I-2	900	7.7	<0.03	12.3	-12.3	75	900	19	1400	6	1500
CS I-3	2000	7.4	2.7	10.7	-8	61	1200	33	1100	6	2000
CS I-4	4800	7.8	<0.03	12.1	-12.1	63	3500	29	2100	8	6100
CS I-5	5000	7.5	<0.03	13.9	-13.9	53	4100	33	2200	14	4700
CS I-6	4600	7.9	<0.03	10.7	-10.7	48	10000	36	-1400	16	7400
CS I-7	5200	7.6	<0.03	12.3	-12.3	63	4200	27	1800	10	7400
CS I-8	6400	7.5	<0.03	9.3	-9.3	63	9300	30	200	7	4800
CS I-9	3400	7.4	0.64	10.7	-10.05	57	2600	35	1200	8	8900
CS I-10	7400	7.7	0.12	10	-9.88	54	8400	38	2400	8	6300
CS I-11	6000	7.5	0.06	9.8	-9.74	60	6300	34	1700	6	8300
CS I-12	3800	7.3	<0.03	6.1	-6.1	73	2900	23	1200	4	13000
CS I-13	9600	7.2	1.08	9.1	-8.02	68	8700	28	3600	4	2300
CS II-1	1600	7.4	7.8	9.9	-2.1	25	1600	65	1000	10	2000
CS II-2	1800	7.5	3.4	11	-7.6	26	2800	62	900	12	1800
CS II-3	1700	7.5	2.9	9.9	-7	26	3400	57	500	17	1700
CS II-4	1600	7.4	5.5	9.8	-4.3	32	2300	52	600	16	1700
CS II-5	1500	7.4	6.3	9.9	-3.6	40	4000	52	-200	8	1200
CS II-6	1200	7.4	7.6	9.3	-1.7	33	1500	59	600	7	1700
CS II-7	1800	7.4	4.2	11.3	-7.1	32	2900	56	600	12	1900
CS II-8	2300	7.4	5.2	10.6	-5.4	35	4300	56	800	9	-
CS II-9	2100	7.5	3.9	11	-7.1	33	3000	56	900	11	1900
CS II-10	1900	-	-	-	-	27	3700	57	900	11	1300
CS II-11	1400	7.6	4.9	10.6	-5.7	32	1800	57	700	16	1100
CS II-12	3500	-	-	-	-	36	5000	50	700	11	1900
CS II-13	1300	7.2	1.3	11.9	-10.6	25	2500	57	1400	14	1100

NOTE: "-" = Not Analyzed, italics indicate calculated value
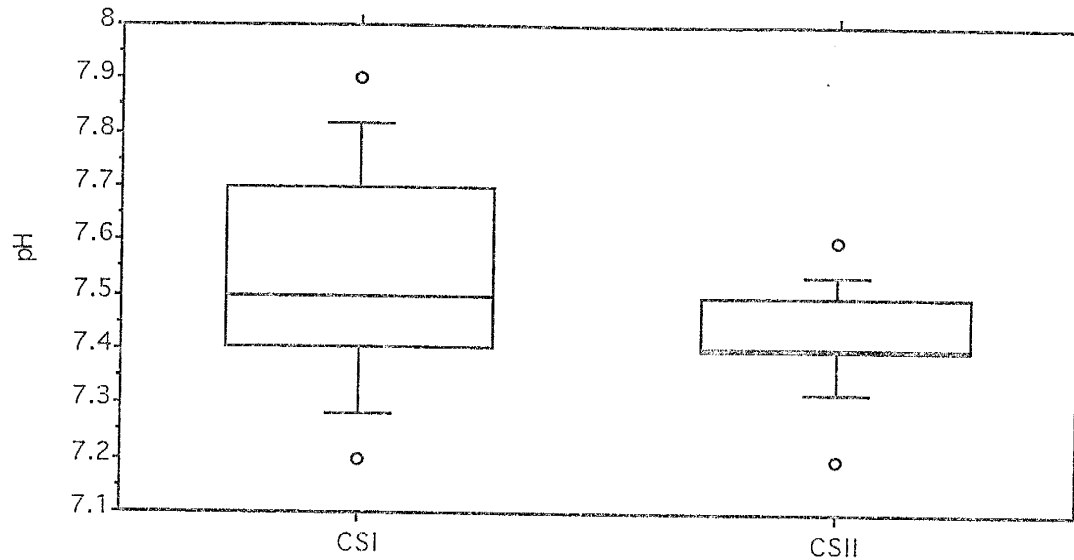
Figure 9: Box and whisker plots showing pH for bulk soil samples from grids CSI and CSII. The box and whisker plots display the data based on percentile ranks. The box shows the 25%, 50% (median), and the 75% ranks. The whiskers show the 10% and 90% ranks. The dots show values less than 10% and greater than 90% ranks. When the dots are displayed, they essentially represent the minimum and maximum values. The distribution represented by the box displays one-half of the data.
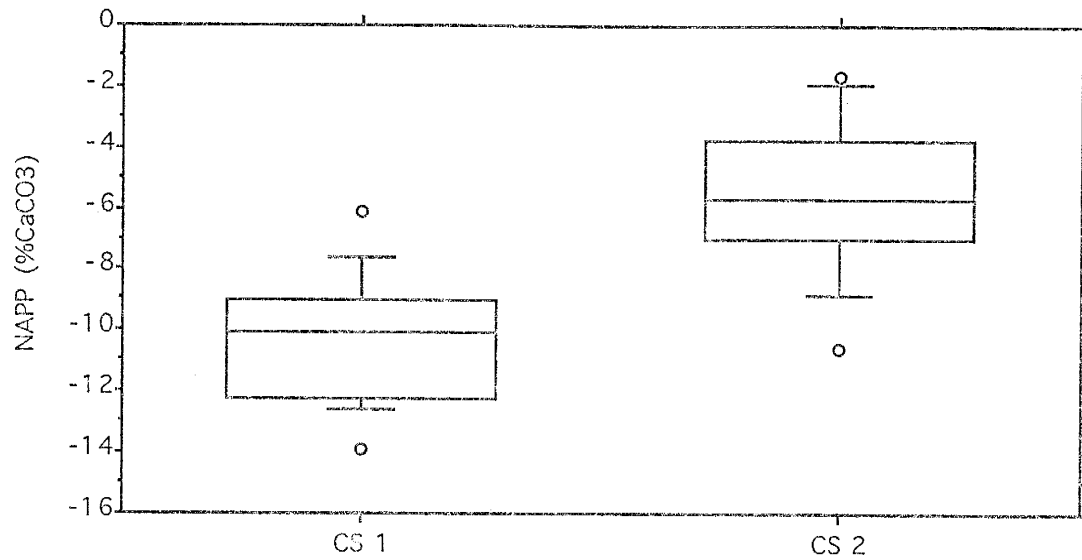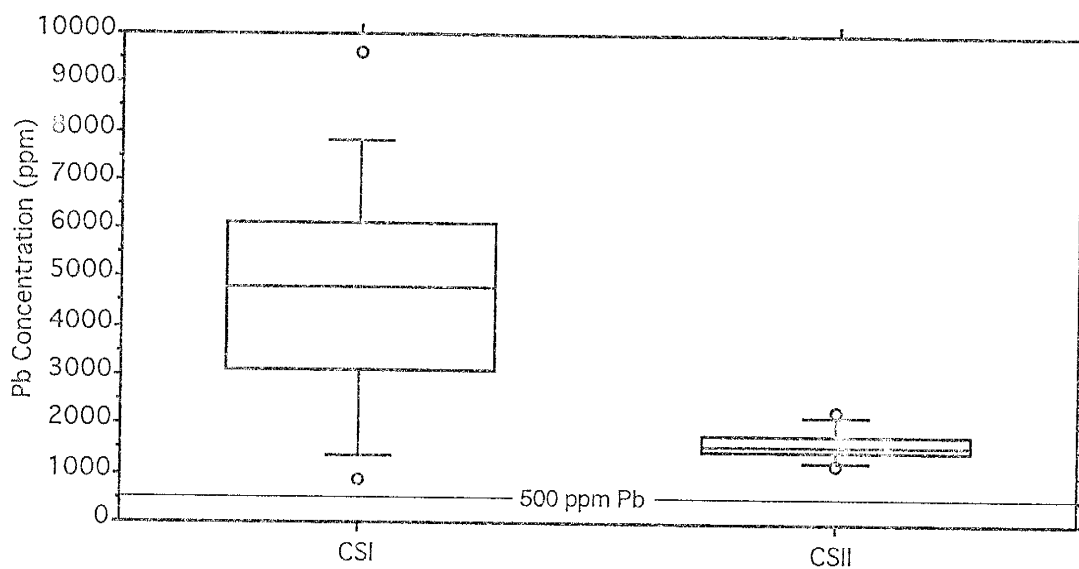
Figure 10: Box and whisker plots showing Net Acid Producing Potential (NAPP) for bulk soils from grids CSI and CSII.

Lead Chemistry In Soils

Pb concentrations for all grid CSI and CS II bulk samples exceed the EPA's "action level" of 500-1,000 ppm Pb in the soils which concurs with the initial XRF survey (Fig 11). The median Pb concentration in grid CS I is 4,800 ppm with a range of 900 to 9,600 ppm with a mean value of 4,662 ppm (Fig 11). In grid CS II, median Pb concentration is 1,600 ppm with a range of 1,200 to 3,500 with a median value of 1,664 ppm (Fig 11).

Pb concentration at the Cuba smelter site is unevenly distributed between sand, silt and clay. The clay-size fraction for CSI on the terrace has the highest Pb concentration at 13,000 ppm, but the coarser material also exceeds the action level with 3,592 ppm calculated for silt and 10,000 ppm determined for sand (Fig 12). The agricultural field sample, CSII, has greater Pb concentrations in the sand-size fraction with values to 5,000 ppm, but all fractions exceed the action level with silt-size fraction to 1,434 ppm and the clay-size fraction to 2,000 ppm (Fig 12).

Pb concentration versus depth was investigated in both sample areas. Shallow trenches were dug to collect soil samples down to 22 cm. The Pb concentration did not decrease with depth. Apparently, the Pb contamination persisted greater than 2' below ground surface, but it could not be addressed during remediation (B. Ridpath, pers. comm. 1994). Two feet was the maximum extent of excavation.

Figure 11: Box and whisker plots showing Pb concentration for bulk soils from grids CSI and CSII. Dashed line indicates action level of 500 ppm Pb in soils as determined by the EPA.
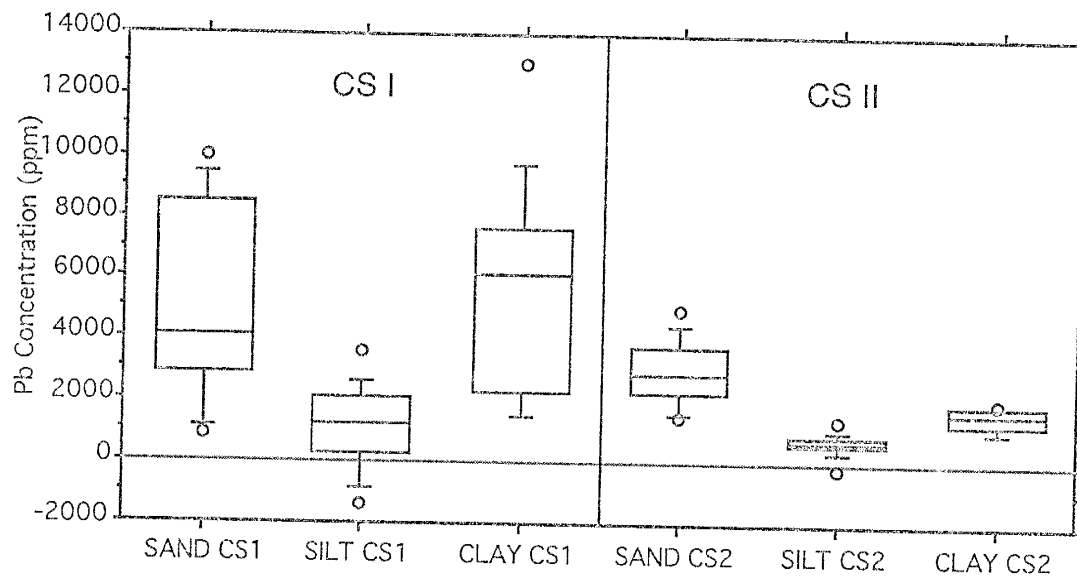
Figure 12: Box and whisker plots showing Pb concentration versus grain size distribution (sand, silt, and clay) in grids CSI and CSII. Pb values are in ppm.

Soil Texture and Mineralogy

The two dominant soils at the Cuba Smelter site are the Arizo, a very stony loamy sand, and the Gila clay loam (USDA, 1988). The Arizo occurs on the terrace (CS-I), and the Gila clay loam occurs in the agricultural field (CS-II).

The soils on the terrace, where the smelter foundations were located, were poorly-sorted gravelly sands with occasional cobbles. The soil horizon on the terrace varied with depth. Silt and clay layers with variable amounts of organic matter were beneath the gravelly sand. These soils supported cacti, shrubs, and grasses. The field samples were sandy silts with clay layers down to 2' below ground surface. The field had grasses growing on the surface.

Many artifacts were found on the surface including broken glass bottles and pottery, bricks, metal scraps, and hand-cut nails. Several small slag piles and an ore pile were deposited around the site. This ore pile was mostly magnetite and some bornite.

In thin-section, the both terrace and field soils had an alveolar structure with abundant irregular pores in a honey-comb pattern resulting in high porosity. This structure is common in the upper horizons of desert soils (Fitzpatrick, 1993). The continuous soil phase is composed of particles ranging from clay to coarse sand. Several root casts and organic debris were identified with the petrographic microscope and EMPA. The matrix seen in thin-section has been analyzed with XRD, and it includes fine-grained quartz, calcite, and clay minerals.

Point-count data show a correlation between samples from the same grid, and a distinct difference between grids. Soils were evaluated for the abundance of grains, matrix, and porosity. Based on ternary plots, the terrace samples tend to group together, and the field samples group together as well. The terrace samples are grain-dominated, whereas the field samples are matrix-dominated (Fig 13).
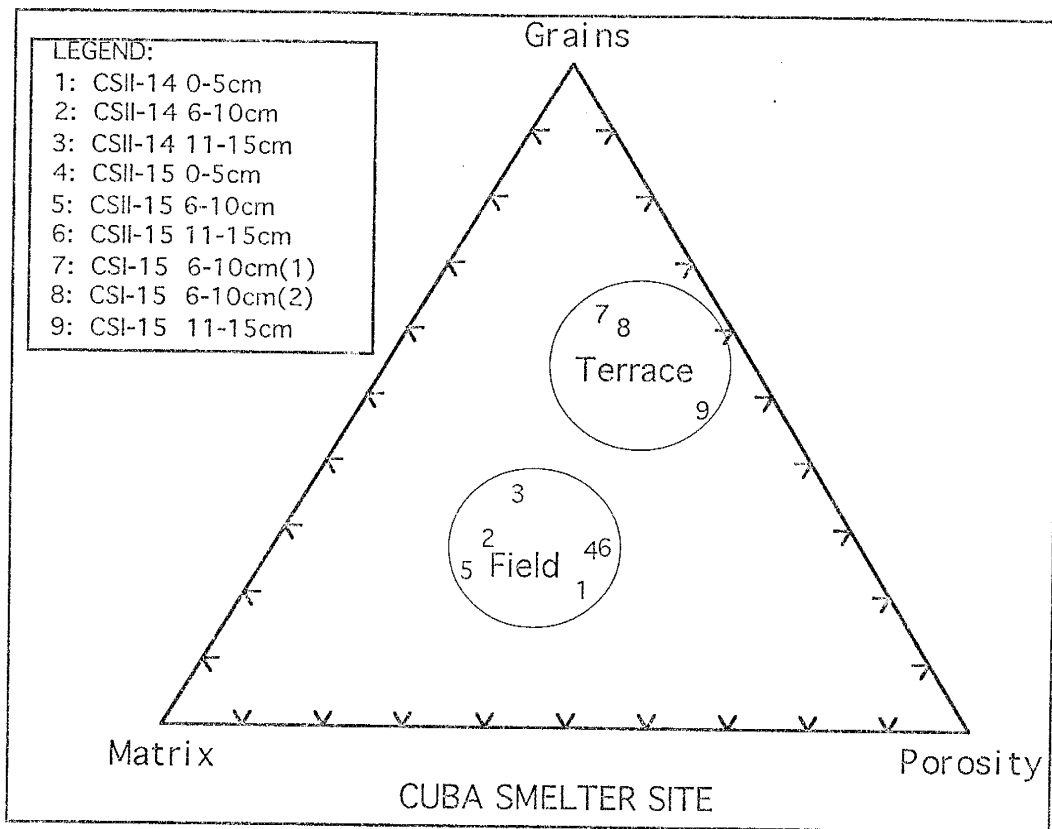
Figure 13: Ternary plot from point-count data for soils at the Cuba smelter site. The axes represent % of components. Note differentiation between field and terrace soils. The field samples are dominated by matrix, whereas the terrace samples are dominated by grains. Both field and terrace samples have a similar porosity ranging from about 30% to about 45%.

Soil-forming minerals were analyzed with the petrographic microscope, XRD, and EMPA. Quartz, feldspar, calcite, and clay minerals constitute the main soil-forming minerals identified by both XRD of <2 mm fraction and EMPA BSE images. The various clay minerals include illite, Ca-smectite, mixed layer illite/smectite, and kaolinite (Table 3). Other minerals identified in the soils with EMPA include galena, pyrite, chalcopyrite, orthoclase, plagioclase, barite, siderite, and apatite.

All grains encountered in the soils are completely surrounded by clay rims, especially evident in Figures 14 and 21. EDS spectra and element maps show the rims probably consist of Ca-smectite, illite, mixed layer I/S, and kaolinite.

Lead Mineralogy

Phases containing Pb at the Cuba smelter site identified by EMPA include galena, slag, and Pb-oxides (Figs 14, 15, 17, 18, 19, 20, 21). Chalcopyrite has Pb disseminated throughout the matrix (Fig 21). Galena is the dominant Pb-bearing phase in the soils.

All galena grains identified were encapsulated. Minerals encapsulating galena are clay minerals, quartz, Fe-oxides, and phosphate crusts (Figs 14, 15, 18). The clay minerals, illite and smectite, are the same as those encapsulating all of the soil particles. Quartz is a gangue mineral that was encapsulating galena in the ore body, and it has maintained this original relationship (Fig 15). The Fe-oxides do not appear authigenic in thin-section because distinct blade-like crystals are evident in BSE images (Fig 15). A phosphate crust was identified around either a galena grain or a dross Pb-particle. The phosphate crust completely encapsulates the Pb particle (Fig 15). This grain was unique because it demonstrates the only phosphate alteration noted during this study.

The galena and pyrite grains do not appear altered, and both show distinct cleavage (Figs 14, 16). Pyrite present in the Cuba smelter soils show no signs of alteration because the cubic structure is quite visible in BSE images without secondary mineral formation (Fig

16). With the exception of the phosphate crust, all sulfide minerals show no signs of secondary mineral formation, but all soil particles including the sulfides are encapsulated by clay minerals.

Slag Texture and Mineralogy

Slag was found scattered around the surface of the site and identified in all soil samples. The slag particles were very angular, looking like obsidian, and exhibited concoidal fractures. Occasionally a spherical particle of slag was encountered. The glassy slag was coated with clay minerals, and it did not appear altered (Figs 19, 20).

Elemental compositions of the glassy slag were investigated using X-ray mapping. The slag matrix is a silicate with numerous impurities. Overall, it contains S, Ca, Si, O, Al, Fe, and Zn, and in some cases Pb. In several samples, the slag matrix also has bands or lamellae that are visible under plane-polarized light (PPL) with the petrographic microscope and on X-ray maps. Under PPL the bands appear as alternating dark and light brown bands. The light brown bands are similar in appearance to the slag matrix seen in samples lacking bands. On X-ray maps the light brown bands are enriched in S, Ca, Si, and O and appear as grey on X-ray maps; whereas the dark bands are enriched in Pb with lesser Zn, Fe, and O and appear white on X-ray maps because of the heavier elements present. Several highly concentrated zones of metals were identified, and all are encapsulated by slag (Fig 20); these are dross textures.

Table 3: Table of semi-quantitative clay mineralogy based on XRD of the <2µ fraction for grid CSI on the terrace. Values are expressed as parts in ten.

SAMPLE #	ILLITE	SMECTITE	I/S	KAOLINITE
CSI-1	5	2	-	3
CSI-2	4.5	0.5	3	2
CSI-3	4	1	1	4
CSI-4	2	1	3	4
CSI-5	9	-	-	1
CSI-6	10	-	-	-
CSI-7	7	-	-	3
CSI-8	7	-	-	3

Notes: "-" = Not Present
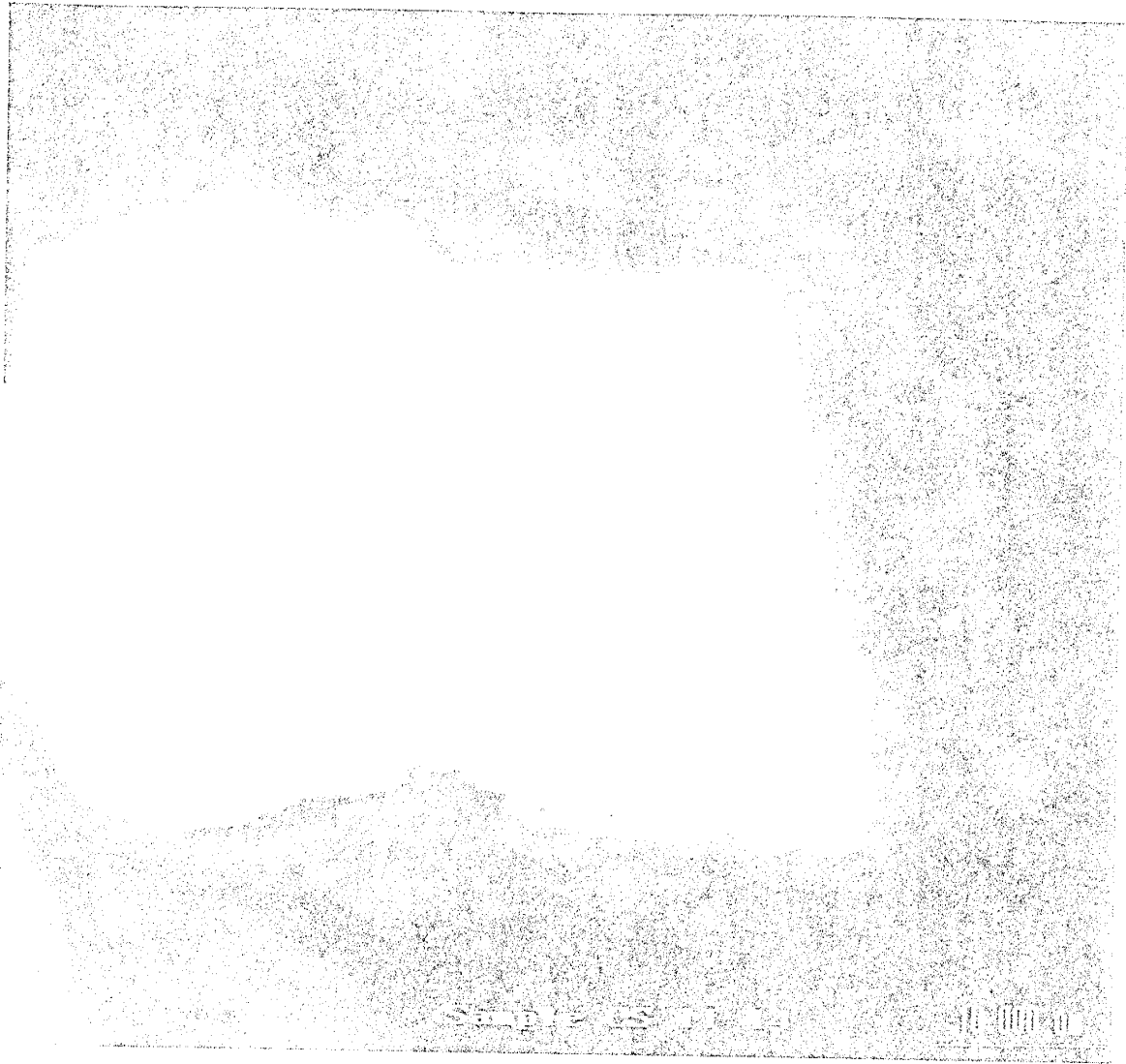I/S = mixed layer illite/smectite

Figure 14: Back-Scattered Electron (BSE) Image showing typical unreacted galena particle with a rim of clay minerals. The grain is approximately 60 microns across or silt-sized. This sample, CSH-14, was collected in the agricultural field from the soils at the Cuba Smelter site, Socorro New Mexico.
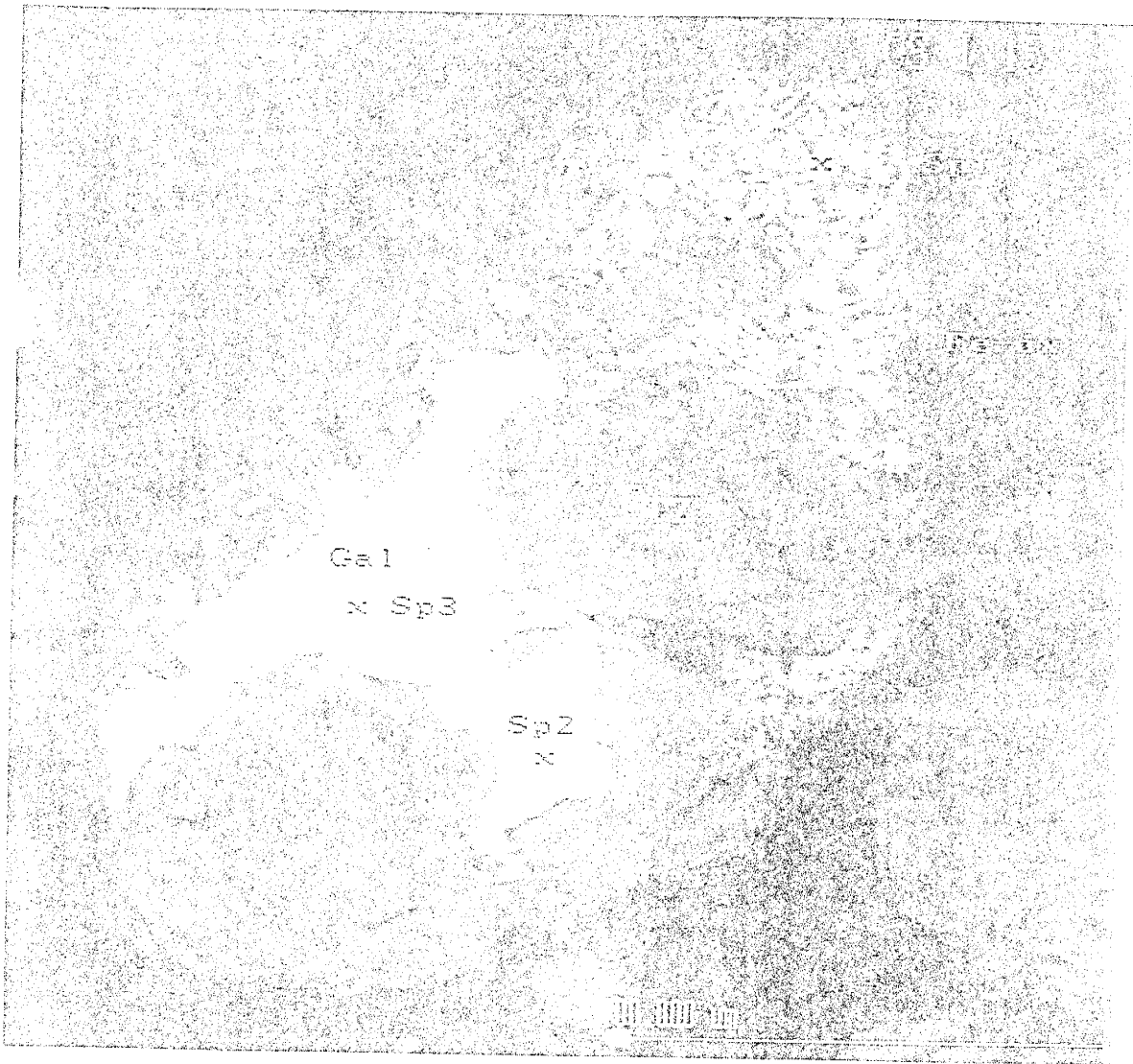Scale Bar = 10 microns

Figure 15: Back-Scattered Electron Image (BSE) showing galena (gal. on image), quartz (qtz. on image), and iron-oxides (Fe-ox. on image). The grain is sand-sized. This sample. CSI-15, was collected on the terrace near the smelter foundation. SP1. SP2. and SP3 are locations of spectra acquisition for mineralogy identification.
Scale Bar = 100 microns

Figure 16: Back-Scattered Electron Image of unreacted sulfide minerals in the soils at the Cuba Smelter site. Socorro New Mexico. The cubic minerals in the center of the image are pyrite grains associated with chalcopyrite and apatite. This sample, CSI-15, which is the same sample as Figure 15, was collected near the smelter foundation. Scale Bar = 1 mm

Figure 17: Back-Scattered Electron (BSE) Image and x-ray maps showing typical minerals in the soils at the Cuba Smelter site, Socorro New Mexico. The BSE image shows feldspars, slag, and clay mineral rims on the larger particles in a fine grained matrix. The composition of the particles may be identified using the x-ray maps for Pb (Fig 17B), sulfur (Fig 17C), and Fe (Fig 17D). Pb is found in the slag grain and in the clay mineral rims (Fig 17B). Sulfur content is high in the slag particle, and it also occurs in the clay mineral rim coincident with Pb indicating galena (Fig 17C). Iron and Pb correspond to each other spatially in the clay rims perhaps indicating Pb is absorbed to iron oxides (Fig 17D).
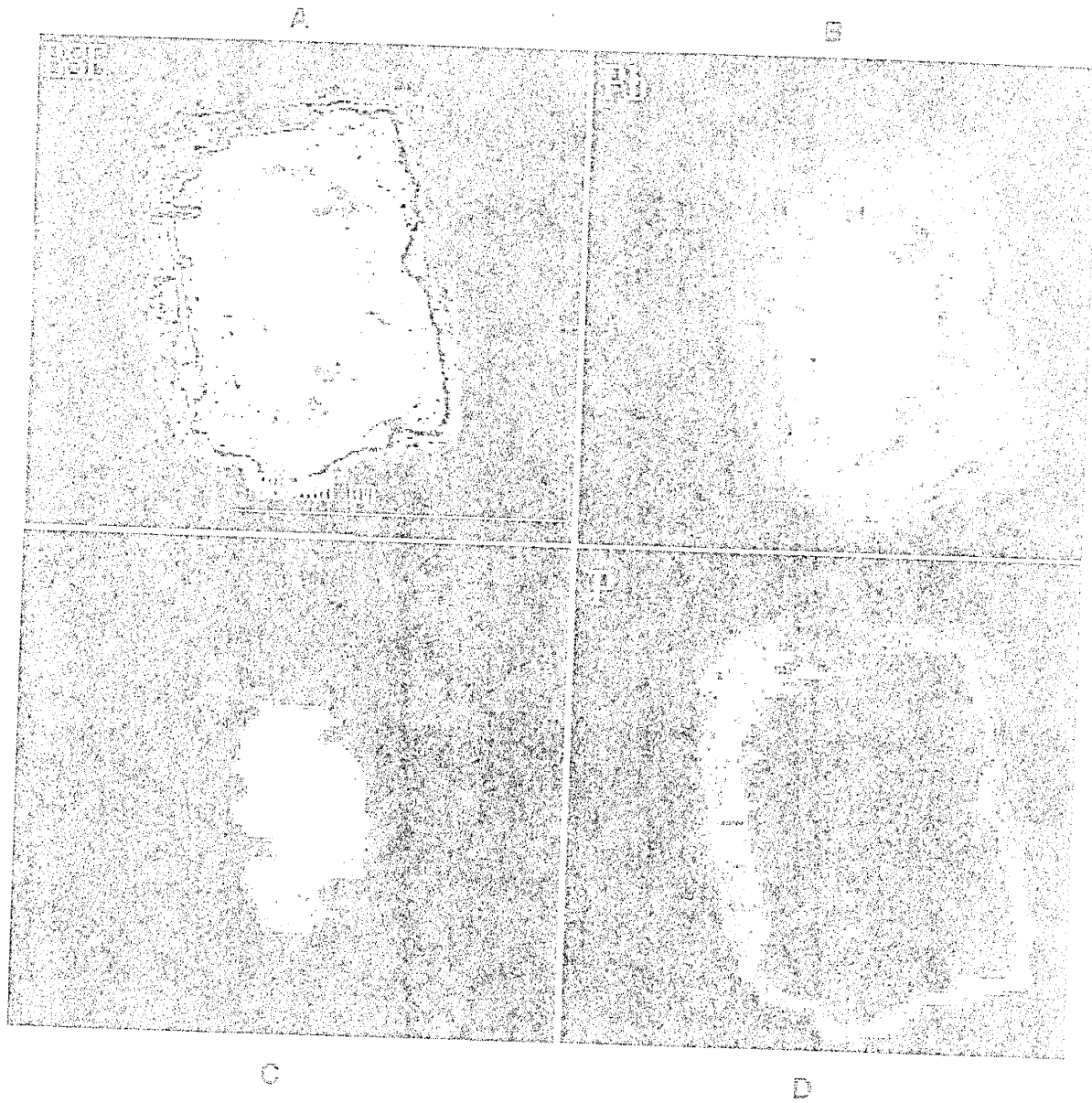
Scale Bar = 100 microns

Figure 18: Back-Scattered Electron (BSE) Image and x-ray maps showing Pb-sulfide mineral armored by a phosphate rim in the soils at the Cuba Smelter site. Socorro New Mexico. This is a unique particle because this was the only galena particle identified with an alteration rim, and the rim consisted of phosphate. The BSE shows an altered grain with a core and two distinct alteration rims (Fig 18A). The Pb content is greatest in center of particle and lessens into the rims (Fig 18B). Sulfur is only present in center of particle which indicates this was originally galena (Fig 18C). Phosphorus (P) is concentrated in outermost rim of particle (Fig 18D).
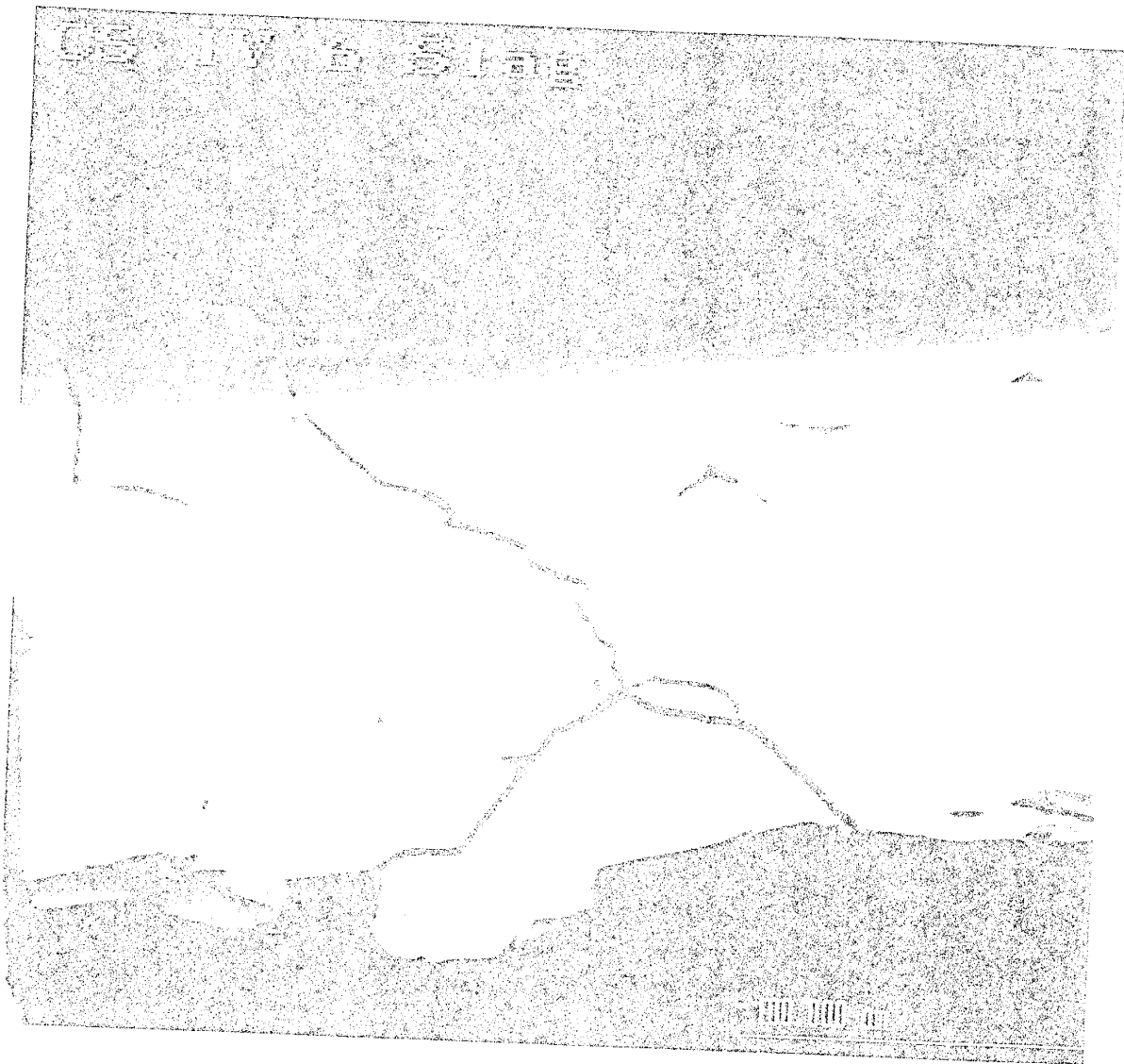Scale Bar = 100 microns

Figure 19: Back-Scattered Electron Image a typical slag particle with an angular shape. Some banding is faintly evident across the grain. This sample was collected near the smelter foundation from the soils at the Cuba Smelter site. Socorro New Mexico. Scale Bar = 100 microns

Figure 20: Back-Scattered Electron (BSE) Image and x-ray maps of a slag particle with a sulfide inclusion. The BSE image (Fig 20A) shows the inclusion in the lower right corner of the image, and a well-defined unaltered contact with the soil matrix. The x-ray maps are for Pb (Fig 20B), sulfur (Fig 20C), and zinc (Fig 20D). These x-ray maps display the composition of the inclusion as a multi-metal sulfide. This inclusion is similar to others identified in the slag, and they are eutectic or dross textures. This sample was collected near the smelter foundation at the Cuba Smelter site, Socorro New Mexico.

Scale Bar = 100 microns
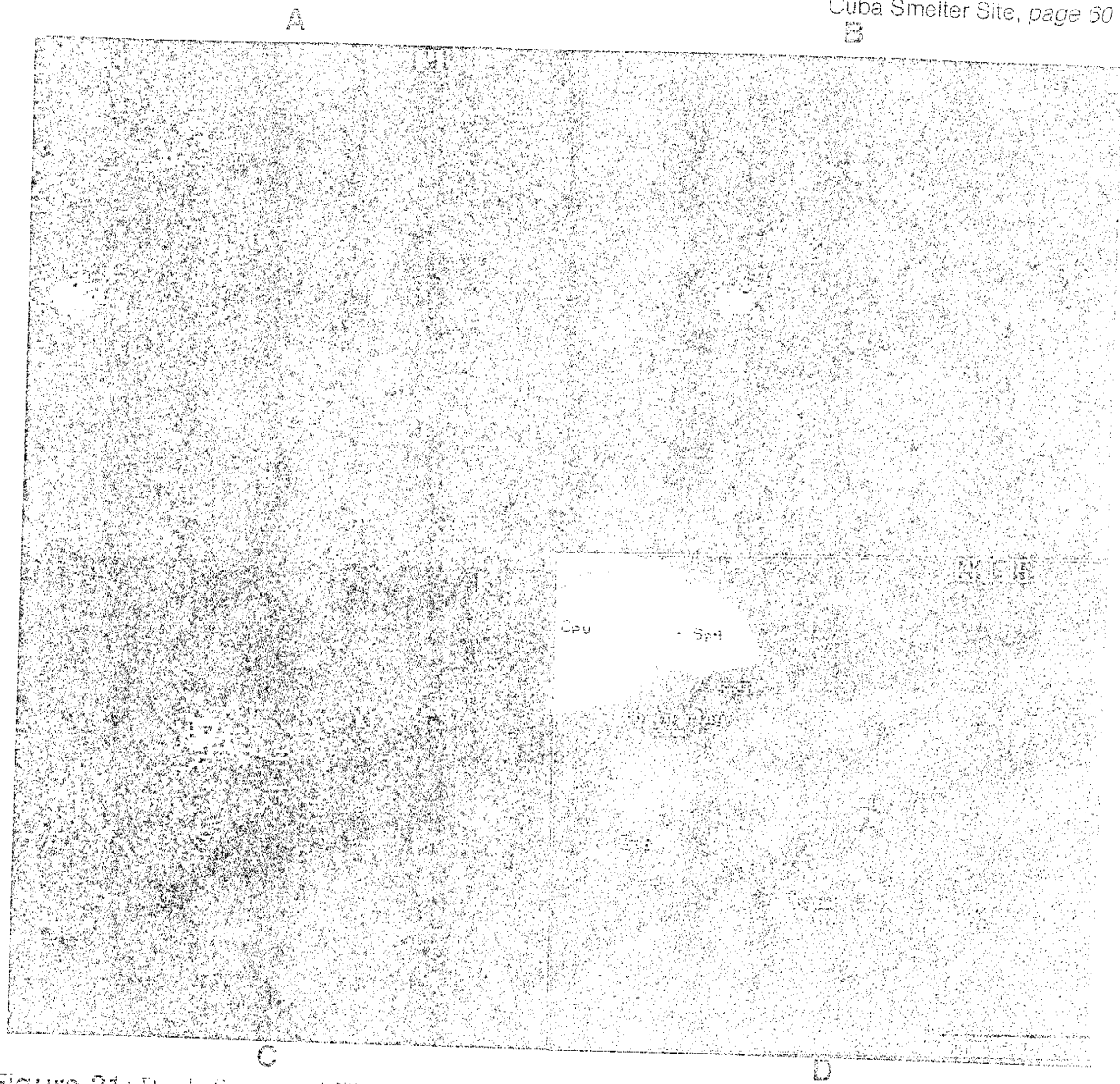
Figure 21: Back-Scattered Electron (BSE) Image and x-ray maps of quartz and chalcopyrite grains with clay mineral rims. The BSE image (Fig 21D) shows a quartz grain (Qtz) in the lower right corner with a 10-micron thick rim (clay). A chalcopyrite grain (Cpy) is in the upper left-hand corner. This grain has a thinner rim, about 2 microns, than the rim on the quartz. These x-ray maps are actually two to three individual maps superimposed. By superimposing the x-ray maps, any correlation between elements appears as a color change. For example, in Figure 21A, Pb is displayed in green and oxygen is displayed in red, so, wherever yellow appears, Pb and oxygen coexist. This yellow area is the location of a Pb-oxide. Pb is also disseminated throughout the chalcopyrite grain. Figure 21B shows the correlation between calcium (Ca) and oxygen. The calcium occurs in a few areas in the rims, so some $CaCO_3$ is evident. The calcium does not appear disseminated in the rim, so Ca-smectite is probably not one of the clay minerals present in the rim. Figure 21C superimposes aluminium (Al), potassium (K), and oxygen. Al and K are found in both rims indicating fine-grained K-spar or illite compose the rims. Scale Bar = 10 microns

DISCUSSION

Origin of Lead-Bearing Phases and Textures

Galena, pyrite, chalcopyrite, and slag in soils at the Cuba smelter site appear to be the result of industrial activities at the site: ore handling, processing, and smelting.

During ore processing and handling, the ore was stored onsite, and then crushed onsite, creating dust particles. Ore crushers and a dust catcher are indicated on the Sanborne Insurance Map seen in Figure 4. This dust, containing unreacted sulfides, probably came in contact with the soils.

Based on chemical and physical characteristics, the unreacted sulfides at the Cuba smelter site are very similar to particles identified as common smelter dusts by Karakus and Hagni (1991). Physically, the particle-size and shape is similar. Most unreacted sulfides at the Cuba smelter site are silt-size and angular in shape. Unreacted sulfide mineralogy is also similar. Both studies identified galena, pyrite, and chalcopyrite.

Karakus and Hagni (1991) identified dust-sized slag particles as well. The slag particles are also very similar. Textures in the slag particles noted at Herculaneum were, also, identified in Cuba smelter site samples.

The eutectic point texture was noted in several Cuba smelter samples. (This eutectic texture is the zone of anomalous metal concentration seen in Figure 20.) The eutectic is the point where two solids and a liquid coexist at the lowest possible melting temperature (Bates and Jackson, 1984). Presumably, these eutectic textures are a remnant of the smelting process and formed when the melt reached the eutectic point. The liquid dross would become a drop within the liquid slag and eventually become trapped as the liquid slag solidified. These eutectic textures are common in slag (Coudurier and others, 1985).

Eutectic compositions in Cuba Smelter site slag include high amounts of Pb and S combined with Cu, Zn, and Fe. The composition is predominantly Pb, Fe, Zn, and S in the eutectic textures at the Cuba smelter site, and these differ from the slag matrix because

they lack the Ca, Si, O, and Al that form the matrix. The eutectic liquid solidified as a sulfide, so this would be considered dross.

Modern slags were investigated by Davis and others (1997) using EMPA, and they noted that fresh slag had concoidal fractures with no signs of devitrification after 5 years of weathering. The fresh slag textures of Davis and others (1997) appear very similar to slag textures from the Cuba smelter site. This is very interesting because the Cuba Smelter slag has been in soils since the turn of the century, and the matrix and dross have not significantly altered.

Besides the eutectic textures in the slag, lamellae containing anomalous metal concentrations were observed. Unfortunately, the lamellae seen in the Cuba Smelter slag were not identified by Karakus and Hagni (1991) or Davis and others (1997). The lamellae texture must be the result of smelter processes and probably formed during the reduction stage when the slag separates from the molten Pb (Coudurier and others, 1985). A set of lamellae may preserve the contact between the molten Pb matte and the slag.

Pb oxides will form during the smelting and sintering processes (Henry and Heinke, 1989). An important observation during x-ray mapping was that Pb occurs with oxygen but never concurrently with sulfur. If Pb and oxygen are associated with each other, then Pb-oxides would exist in the soils at the Cuba smelter site. These Pb-oxides are always associated with clay rims and are probably absorbed to clay minerals. Their presence is not unusual, and the Pb-oxides are probably sinter particles which passed through the smelter stacks and became deposited on the soils.

Grain-Size Distribution of Lead-Bearing Phases

Pb distribution was not uniform between the two sampling areas. The terrace soils have a large range of Pb values, reflecting the heterogeneous nature of the contamination.

A narrower range of Pb values occurs with the field samples probably because they were homogenized by the anthropogenic activities of plowing, irrigation, and harvesting.

Distribution of Pb also varied between the two sampling areas. The terrace samples exhibit a larger distribution of Pb concentrations versus grain-size compared to the field samples. Clay fractions have higher median Pb concentrations than silt and sand sizes for the terrace soils, and the clay is the smallest portion of the soil by mass. Sand fractions have the highest median Pb concentrations as opposed to the clay and silt sizes in the field soils, and sand is the lowest percent of soil by mass.

The differences between the field and terrace are probably related to both smelter and farming activities. The terrace samples would have probably received more airfall of smelter emissions (Pb-oxides) due to prevailing winds generally blowing out of the southwest. Modern smelters have upwards of 500 pounds of emissions per ton of processed ore, so this could be a significant amount of accumulation. The ore crushers and dust catcher were located on the terrace and these obviously created dust particles of silt and clay sizes. These emissions and dusts would remain in the terrace soils because few reactions are occurring to remove the Pb. The field soils would have received similar emissions and dusts, but not to the same degree as the terrace. The field soils have also been reworked as an agricultural field. These activities would plow particles deposited on the soil surface deeper into the profile essentially homogenizing the contamination throughout the depth of the plow. This homogenization of field samples is evident by the lower median values for Pb in bulk, sand, and clay samples. Irrigation may have increased dissolution of particles, but galena grains from the field were not altered in the surface samples collected.

Austin and others (1993a, 1993b), also show a correlation between clay-size fractions and high Pb concentrations at the nearby Billing Smelter in Socorro, New Mexico in samples collected downwind from that smelter. These samples are comparable to the

terrace samples at the Cuba smelter: the greatest Pb concentration existed in the finer grain-size fractions, and these fine fractions were present in the lowest percentage. When considering Pb distribution, the field samples are probably different than the terrace samples due to farming activities in the field.

Lead-Distribution in the Slag Samples

Slag is an important Pb-bearing phase in Cuba smelter site soils. The slag may act to reduce availability through encapsulation of metals and Pb by refractory glass. The glass encapsulates unusual metal phases which are probably eutectic textures or dross. This encapsulation reduces exposure of these metal enriched zones to the soil solutions. The Pb present in the slag, dross, disseminated, and lamellae, will have a lowered availability due to the insoluble matrix.

Soils from the nearby Billing Smelter also contained slag (Austin and others 1993a, 1993b). The Billing's slag was characterized for mineralogy. Slag from the Cuba Smelter could have the same mineralogy as the slag from the Billing Smelter assuming similar technology and techniques were used at the two smelters in conjunction with similar ores. Billing Smelter slag was analyzed by Austin and others (1993b) with XRD. They demonstrated that the Billing slag mineralogy matches akermanite ($Ca_2(Mg,Fe,Al)Si_2O_7$), a member of the meillite group. X-ray mapping of Cuba smelter slag shows that the slag is dominantly Si and O with various impurities including Ca, Fe, and Mg, so this slag may also match the mineralogy of akermanite.

Implications for Lead Availability
Soil Chemistry and Lead Mineralogy

Soils at the Cuba smelter site probably immobilized Pb phases thus reducing Pb availability, which is similar to the Billing smelter site (Austin, 1993a). The soil pH is

alkaline and has a negative net acid producing potential (NAPP), not to mention a potentially high CEC from the presence of smectite, illite, mixed layer illite/smectite and kaolinite. Secondary precipitation products, which indicate dissolution and subsequent precipitation, such as jarosite were not detected. So, Pb in the chemical environment at the Cuba smelter site does not appear to have dissolved, and any dissolved metals would probably be adsorbed to clay minerals as observed in the soils.

The fact that galena has not been altered means it is either stable or metastable under present conditions. Galena typically forms in reducing conditions when it is precipitated in an ore deposit (Garrels and Christ, 1965). The galena should not be stable in an oxidizing soil, but anglesite should be stable. Generally, unsaturated soil will be an oxidizing environment where a constant flux of atmospheric oxygen is available as a reactant (Faure, 1991). The Cuba smelter soils should be an oxidizing environment because they have a low moisture content and are exposed to the atmosphere. Galena has the potential to oxidize, but no signs of anglesite alteration were identified. Normally, sulfides will oxidize in the presence of oxygen and water, but oxidation has not occurred in the soils at the Cuba smelter site for nearly a century. Pyrite is present in the Cuba smelter soils, but it, also, shows no signs of alteration. The galena is probably metastable under present conditions and could begin to alter if soil moisture increased.

Unlike previous studies concerning availability, galena in the Cuba smelter soils did not oxidize to anglesite. Mine-impacted soils from Butte, Montana containing galena have a reduced availability due to encapsulation by anglesite, gangue minerals, and precipitation of jarosite (Davis and others, 1992; Ruby and others, 1992; Davis and others, 1993). Instead, at the Cuba smelter site, galena is encapsulated by clay minerals and gangue minerals reducing availability.

The Cuba smelter soils have reduced Pb availability due to Pb mineralogy within and encapsulation by slag. Slag encapsulates other Pb phases, further reducing availability

due to the insoluble nature of the slag. The reduced availability of slags was demonstrated using *in-vivo* tests by Davis and others (1997), and they estimated that several modern slags had a reduced bioavailability of Pb ranging from 1.5% to 25.5% of total Pb content. Slag at the Cuba smelter site encapsulates eutectic textures with high metal concentrations, and disseminated Pb. This encapsulation must reduce the availability of the Pb present in the slag. The slag appears unreactive and show no signs of devitrification. If the slag is unreactive then Pb within it is essentially unavailable.

Pathways and Health Issues

Considering the pathways presented by Sanders (1990), the onsite/direct contact has the greatest potential health threat. The other pathways have lowered health threats. Groundwater is not likely to be affected because the Pb is encapsulated, and samples were collected by Sanders (1990). The only detected Pb in groundwater was in unfiltered samples from the EPA well, but filtered samples had no detectable Pb levels. Filter size was not indicated. Sub-micron filters (<0.45 μ) are commonly used for groundwater samples, and any detectable Pb in filtered samples is considered a dissolved phase. Since Pb was not detected in filtered samples, the Cuba smelter site Pb is insoluble and is not being dissolved by groundwater. Surface water may have been an issue because the site lies in a 500 year floodplain of the Rio Grande river, and the grains could be physically transported downstream before remediation. The airborne as a pathway for release would pose the same risk as direct contact, because airborne pathways involve the physical transport of fine particles. Even if grains were transported offsite, they would remain encapsulated and retain low solubilities acting to reduce Pb availability.

Prior to remediation, the ingestable (<100 micrometer) fraction of the soils may have posed a health threat, especially to young children who may have played in and, inadvertently, ingested soil at the abandoned smelter site. This is the onsite/direct contact

pathway. Though the Pb availability has been reduced by encapsulation, acidic GI tract fluids with a pH = 2 may reverse adsorption of clay minerals to the galena in favor of hydrogen ions, a phenomenon that occurs in soils (Zimdahl and Skogerboe, 1977). Once the clay armor is removed, galena's availability may actually increase. Fortunately, galena solubility is very low in the GI tract over the two hour residence time (Davis and others, 1992; Ruby and others, 1992; Davis and others, 1993).

CONCLUSIONS

- Prior to remediation Pb levels in the abandoned Cuba smelter soils were elevated above the EPA's Pb action level of 500 - 1,000 ppm in soils. These concentrations may have posed a health threat to humans, but the threat was minimal. Pb availability is controlled by soil chemistry, Pb mineralogy, and moisture content. Whatever health threat was present at the site has been addressed by remediation.

- Several Pb phases exist at the Cuba smelter site. Unaltered galena dominated the Cuba smelter site Pb assemblage. The dry alkaline soils represent an environment in which the galena and other Pb phases are not soluble. Galena was observed encapsulated by unreactive and inert phases (pyrite and quartz) and, also, clay mineral rims. Other Pb phases include smelter-derived slag and Pb-oxides, which were also coated by clay mineral rims.

- Based on the availability and distribution of Pb at the Cuba smelter site, the release of hazardous material was possible before remediation, but the Pb has a reduced availability due to encapsulation. The lack of pyrite and galena alteration indicates waste material was not soluble under present soil conditions. Groundwater and surface water pathways were not threatened.

- The pathways most likely for release were airborne and-or direct/onsite contact. Socorro experiences high winds and is arid, so the silt and clay fractions could have been transported offsite. Of course, the Pb phases would probably remain encapsulated. While the onsite/direct contact pathway may threaten children who inadvertently ingest the soil, the lower availability of Pb should increase the action level appropriately, and encapsulation would reduce availability in the GI tract.

- Overall, encapsulation of Pb particles minimized the health threat of Pb in Cuba smelter site soils. Remediation addressed the pathways of direct contact by fencing the site and airborne transport by soil removal and addition of a soil cover. Certainly the presence of Pb at elevated levels required action at the Cuba smelter site, but an alternative strategy including a site-specific action level for Pb in soils could have been adopted. Phosphate amendments probably would have been successful in lowering Pb availability. Obviously, remediation of the slag pile was deemed unnecessary because it "passed" a TCLP extraction test, so more tests on the soils should have been performed to determine availability.

- Metals in soils must be well characterized during site evaluation including a study of availability before a costly clean-up occurs. A study of blood lead correlated with Pb levels in soils should have been critical in determining the necessity of cleaning up this site.

REFERENCES

Austin GS, Brandvold LA, Hawley JW, and Renault J (1993a) Lead contamination at old smelter sites in Socorro, New Mexico: Part I. Particle size and depth of contamination. Mining Engineering 45: 389-395

Austin GS, Brandvold LA, and Renault J (1993b) Lead contamination at old smelter sites in Socorro, New Mexico: Part II. Laboratory studies. Mining Engineering 45: 396-401

Baker TG (1993) Mobility of heavy metals in soils and tailings at the Hanover and Bullfrog tailings sites, Silver City, New Mexico. New Mexico Bureau of Mines & Mineral Resources, Open-File Report 393

Bates RL and Jackson JA (1984) Dictionary of Geological Terms. Third edition. Anchor Press/Doubleday

Brandvold LA, Popp BR, and Swartz SJ (1996) Lead content of plants and soils from the three abandoned smelters in and near Socorro, New Mexico. Environmental Geochemistry and Health 18: 1-4

Cepeda JC (1987) Relative mobility of lead and copper in soils: an example from the Bonanza district, Saguache county, Colorado. Texas J of Sci 39:29-35

Chaney RL (1988) Metal speciation and interaction among elements affect trace element transfers in agricultural and environmental food chains in Metal Speciation: Theory, Analysis, and Application (eds) Kramer JR and HE Allen pp219-260

Coudurier L, Hopkins DW, and Wilkomirsky I (1985) Fundamentals of Metallurgical Processes Second edition. Pergammon Press

Davis A, Ruby MV, Goad P, Eberle S, and Chryssoulis S (1997) Mass balance on surface-bound, mineralogic, and total lead concentrations as related to industrial aggregate bioaccessility. Environ. Sci. Technol. 31: 37-44

Davis A, Drexler JW, Ruby MV, and Nicholson A (1993) Micromineralogy of mine wastes in relation to lead bioavailability, Butte, Montana. Environ. Sci. Technol. 27: 1415-1425

Davis A, Ruby MV, and Bergstrom PD (1992) Bioavailability of arsenic and lead in soils from the Butte, Montana, mining district. Environ. Sci. Technol. 26: 461-468

Elliott HA, Liberati MR, and Huang CP (1986) Competitive adsorption of heavy metals in soils. J of Environ. Qual. 3:214-219

EPA (1994) Drinking water standards and health advisories table.

EPA (1993) Administrative Record File-Removal Action-Site Name: Cuba Smelter, United States Environmental Protection Agency

Evans LJ (1989) Chemistry of metal retention by soils. Environ. Sci. Technol. 23: 1047-1056

Eveleth R W (1983) Gustav Billing, the Kelly Mine and the Great Smelter at Park City, Socorro County, New Mexico. Guidebook 34 New Mexico Geological Society, pp 89-95

Ewers U and Schlipköter H (1991) Lead in Metals and Their Compounds in the Environment ed. E Merian p 971-1014

Faure (1991) Principles and Applications of Inorganic Geochemistry, J Wiley & Sons

Fitzpatrick EA (1993) Soil Microscopy and Micromorphology , J Wiley & Sons

Freeman GB, Johnson JD, Killinger JM, Liao SC, Feder PI, Davis AO, Ruby MV, Chaney RL, Lovre SC and Bergstrom PD (1992) Relative bioavailability of lead from mining waste soil in rats. Fundam. Appl. Toxicol. 19: 388-398

Fuller CC and Davis JA (1987) Processes and kinetics of Cd sorption by a calcareous aquifer sand. Geochimica et Cosmochimica Acta 51:1491-1502

Garrels RM and Christ CL (1965) Solutions, Minerals, and Equilibria. Harper and Row

Grogin DM and Merians D (1997) 1996 Blood lead levels, prevalence rates and screening guidelines for children in New Mexico. State of New Mexico, Department of Health, Epidemiology Report: May 1997

Gunn AM, DA Winnard, and DTE Hunt (1988) Trace metal speciation in sediments and soils in Metal Speciation: Theory, Analysis, and Application (eds) Kramer JR and HE Allen

Henry JG and Heinke GW (1989) Environmental Science and Engineering. Prentice-Hall pp 491-493

Johnson PS and Deeds JL (1995a) A site conceptual model of environmental issues at the Pecos Mine: Guidebook 46 New Mexico Geological Society, pp 41-42

Johnson PS and Deeds JL (1995b) Summary of environmental issues at El Molino Mill, North-Central New Mexico: Guidebook 46 New Mexico Geological Society, pp 319-322

Karakus M and Hagni RD (1991) Reflected light and electron microscopic characterization of dust and lead from lead and coppr smelters. in Reddy RG, Imrie WP, and Queneau PB (eds.) Residues and Effluents-processing and Environmental Considerations: The minerals, metals, and materials society pp127-142

Kargbo DM (1994) Chemical contaminant reactions and assessment of soil cleanup levels for the protection of groundwater. Environmental Geology 23:105-113

Koch RJ and Barkmann G (1995) Summary of environmental sampling at forest service roads and campgrounds near Cowles, New Mexico: Guidebook 46 New Mexico Geological Society, pp 43-44

Kooner ZS (1993) Comparitve study of adsorption behavior of copper, lead, and zinc onto goethite in aqueous systems. Environmental Geology 21:242-250

Kowalinski S and Weber J (1988) A micromorphological study of a brown leached soil profile polluted by the copper smelter Leginca (Poland) since 1959. Catena 15:303-317

Link TE, Ruby MV, Davis A, and Nicholson AD (1994) Soil lead mineralogy by microprobe: An interlaboratory comparison. Environ. Sci. Technol. 28: 985-988

McKee JD and S Wilson (1974) Socorro Photographer: Joseph Edward Smith 1858-1936. Socorro County Historical Society

McLemore VT, Brandvold LA, Hossian AM, and Pease TC (1995) The effect of particle size distribution on the geochemistry of stream sediments from the upper Pecos River, San Miguel County, New Mexico: Guidebook 46 New Mexico Geological Society, pp 323-329

Moore DM and Reynolds RC (1989) X-Ray Diffraction and the Identification and Analyses of Clay Minerals

Nieman CL (1972) Spanish times and boom times toward an architectural history of Socorro, New Mexico. Socorro County Historical Society

NIST (1992a) SRM 2710: Montana Soil: Certificate of analysis. National Institute of Standards & Technology

NIST (1992b) SRM 2711: Montana Soil: Certificate of analysis. National Institute of Standards & Technology

Osburn GR (1984) Geology of Socorro County. New Mexico Bureau of Mines and Mineral Resources, Open-File Report 238, 13 pp

Pace CB and DiGiulio RT (1987) Lead concentrations in soils, sediment and clam samples from the Pungo river peatland area of North Carolina, USA. Environ. Poll. 43:301-311

Renner R (1995) When is lead a health risk? Environ. Sci. Technol. 29:256A-261A

Rimstidt JD, Chermak JA, and Gagen PM (1994) Rates of reactions of galena, sphalerite, chalcopyrite and arsenopyrite with Fe(III) in acidic solution. in Alpers CN and Blowes DW (1994) Environmental Geochemistry of Sulfide Oxidation. ACS Symposium Series 550

Ruby MV, Davis A, Kempton JH, Drexler JW, and Bergstrom PD (1992) Lead bioavailability: Dissolution kinetics under gastric conditions. Environ. Sci. Technol. 26:1242-1248

Ruby MV, Davis A, and Nicholson A (1994) In situ formation of lead phosphates in soils as a method to immobilize lead. Environ. Sci. Technol. 28: 646-654

Sanders M (1990) Screening site investigation, Cuba Smelter, Socorro, New Mexico: Unpublished report of the Environmental Improvement Division, Santa Fe, New Mexico, 20 pp (with appendixes)

Sandstead (1988) Interactions that influence bioavailability of essential metals in humans, in Metal Speciation: Theory, Analysis, and Application (eds) Kramer JR and HE Allen

Schmitt MDC, Trippler DJ, Wachtler JN, and Lund GV (1988) Soil lead concentrations in residential Minnesota as measured by ICP-AES. Water, Air and Soil Poll. 39:157-168

Schulthess CP and Huang CP (1990) Adsorption of heavy metals by silicon and aluminum oxide surfaces on clay minerals. Soil Science Society of America Journal 54:679-688

Smith R, Walter G, Arkle T and Sobek A (1974) Mine spoil potentials for soil and water quality. EPA-670/2-74-070

Sposito G (1989) The Chemistry of Soils. Oxford University Press
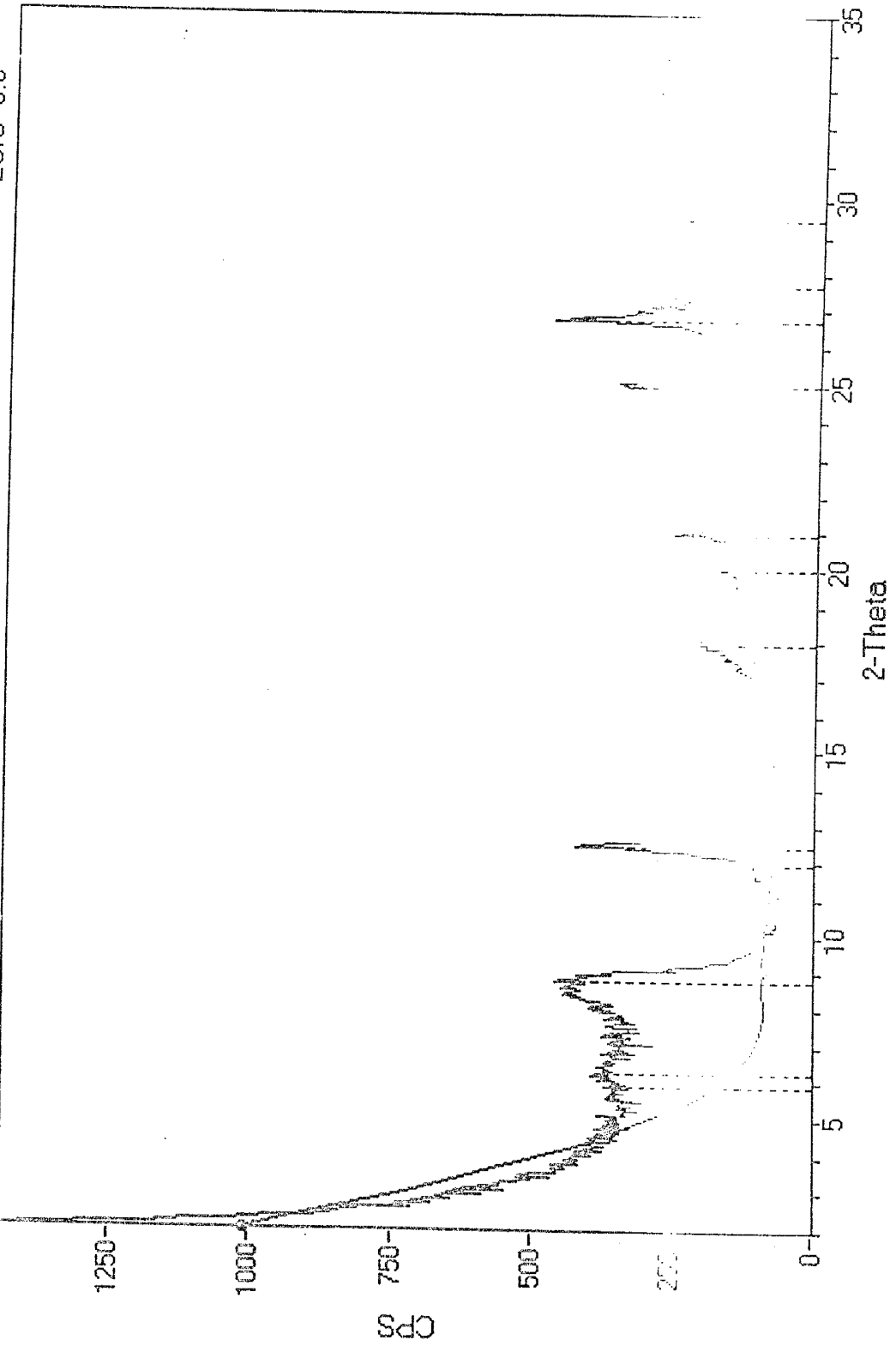
USDA (1988) Soil Survey of Socorro County

Williamson MA and Rimstidt JD (1992) Correlation between structure and thermodynamic properties of aqueous sulfur species. Geochimica et Cosmochimica Acta 56:3867-3880

Williamson MA and Rimstidt JD (1994) The kinetics and electrochemical rate-determining step of aqueous pyrite oxidation. Geochimica et Cosmochimica Acta 58:5443-5454
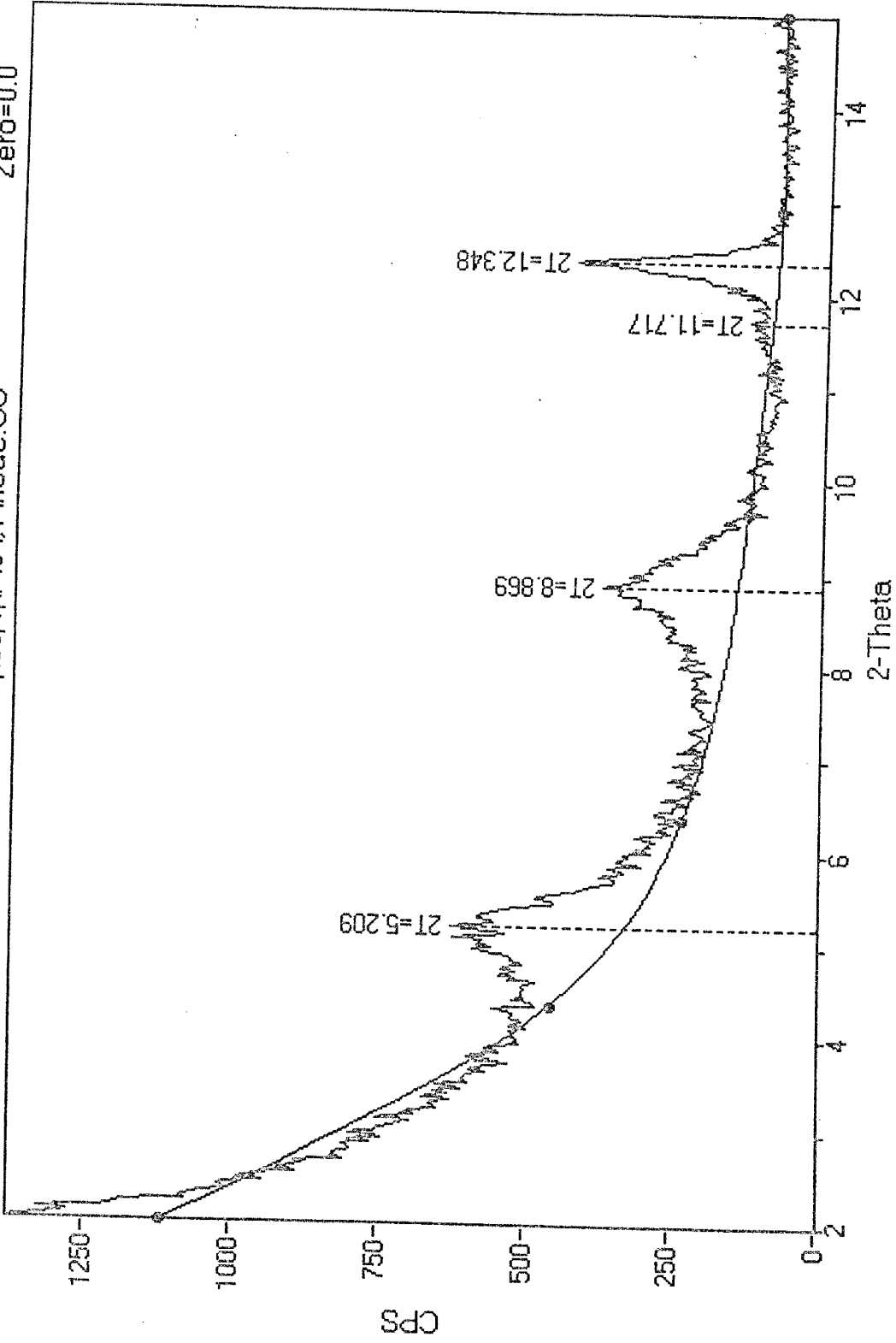
Zimdahl RL and Skogerboe RK (1977) Behavior of lead in soil. Environ. Sci. Technol. 11:1202-1207
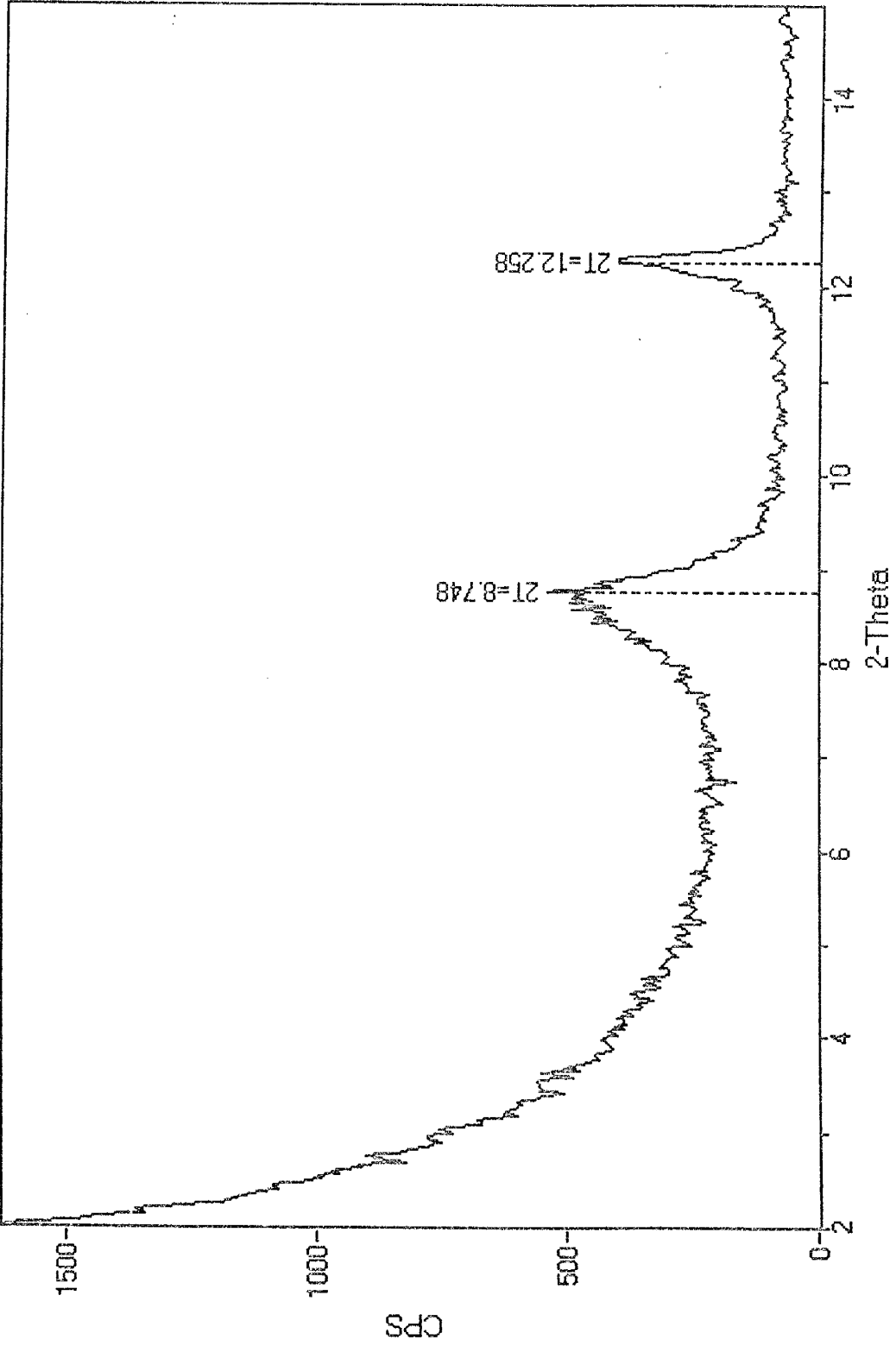
Appendix: Diffraction Patterns of Oriented Clay Slides

ID: CSI-3

File: CSI-3.MDI

Scan: 2-35/.03/1/#1101, Anode:CU

Zero=0.0
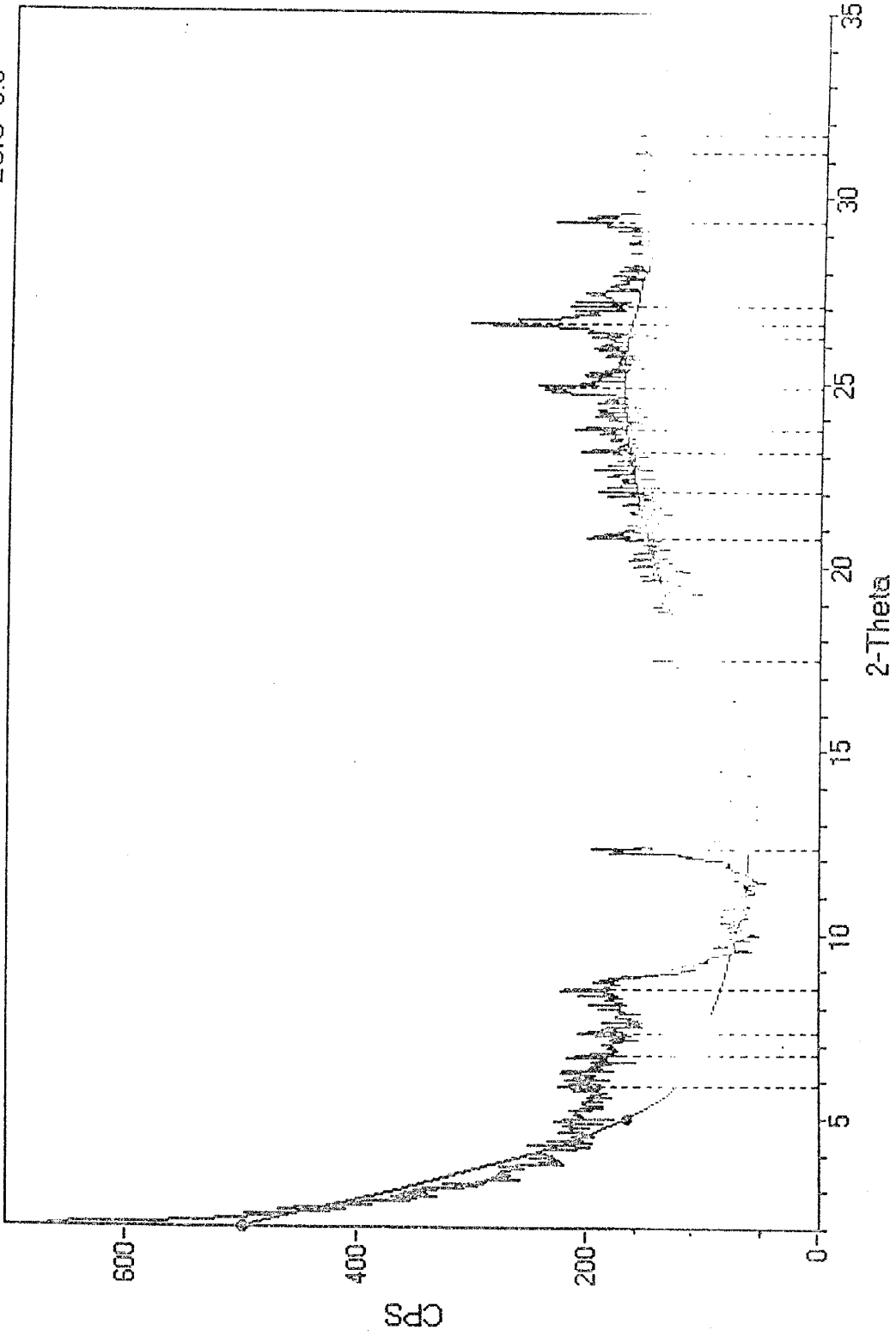
CPS

1250

1000

750

500

2??

0

5 10 15 20 25 30 35

2-Theta

ID: CSI-3G

Scan: 2-14.99/.03/1/#434, Anode:CU

Zero=0.0

File: CSI-3G.MDI
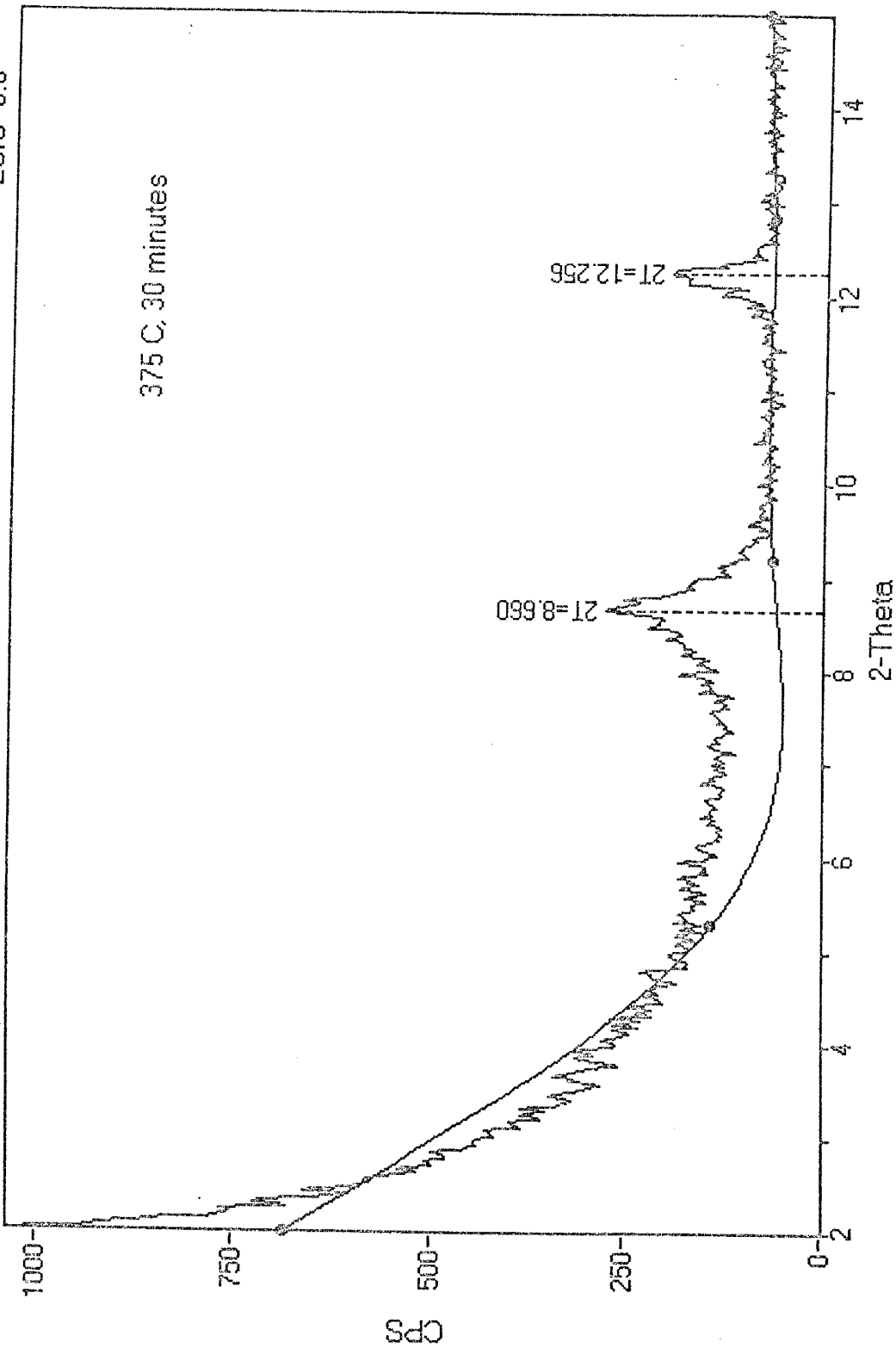
2T=12.348

2T=11.717

2T=8.869

2T=5.209

CPS

2-Theta

ID: CSI-3H
File: CSI-3H.MDI

Scan: 2-14.99/.03/1/#434,Anode:CU

Zero=0.0

2T=12.258

2T=8.748

2-Theta

CPS

1500

1000

500

0

2   4   6   8   10   12   14

ID: CSI-4   Scan: 2-35/.03/1/#1101,Anode:CU   Zero=0.0
File: CSI-4.MDI

CPS

600
400
200
0

5   10   15   20   25   30   35
2-Theta

ID: CSI-4G
File: CSI-4G.MDI

Scan: 2-14.99/.03/1,#434,Anode:CU
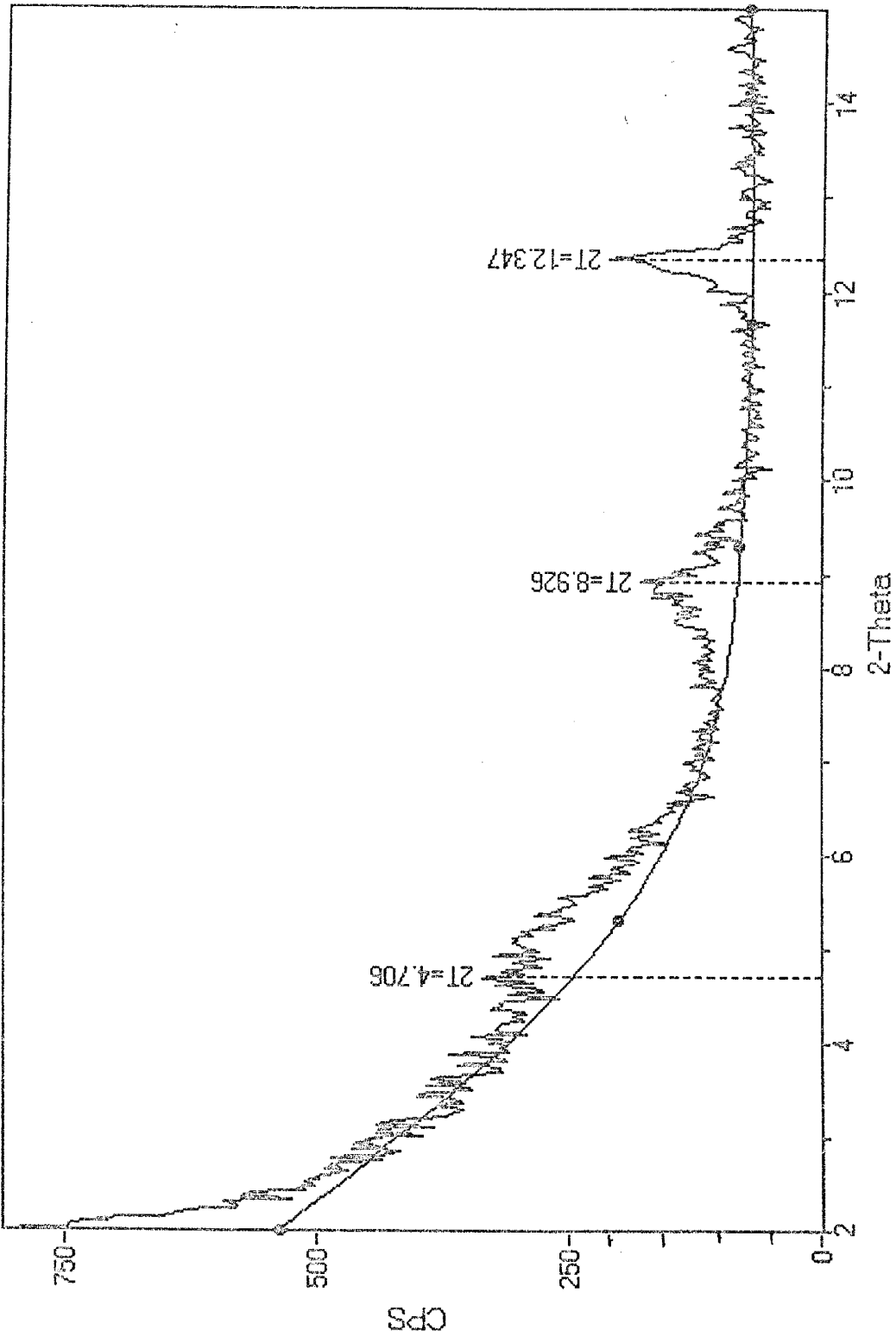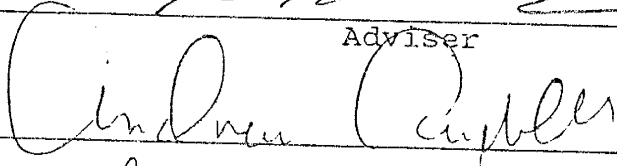
Zero=0.0

2T=12.347

2T=8.926

2T=4.706

CPS

750

500

250

0

2   4   6   8   10   12   14

2-Theta

ID: CSI-4H   Scan: 2-14.99/03/1/#434, Anode:CU   Zero=0.0
File: CSI-4H.MDI

375 C, 30 minutes

2T=8.660

2T=12.256

CPS

2-Theta

ID: CSl6G
File: CSl6G.MDI

Scan: 2-24.98/.03/1/#787, Anode:CU

Zero=0.0

Glycolated

CPS

2-Theta

1500

1000

500

0

5

10

15
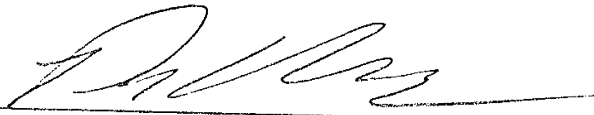
20
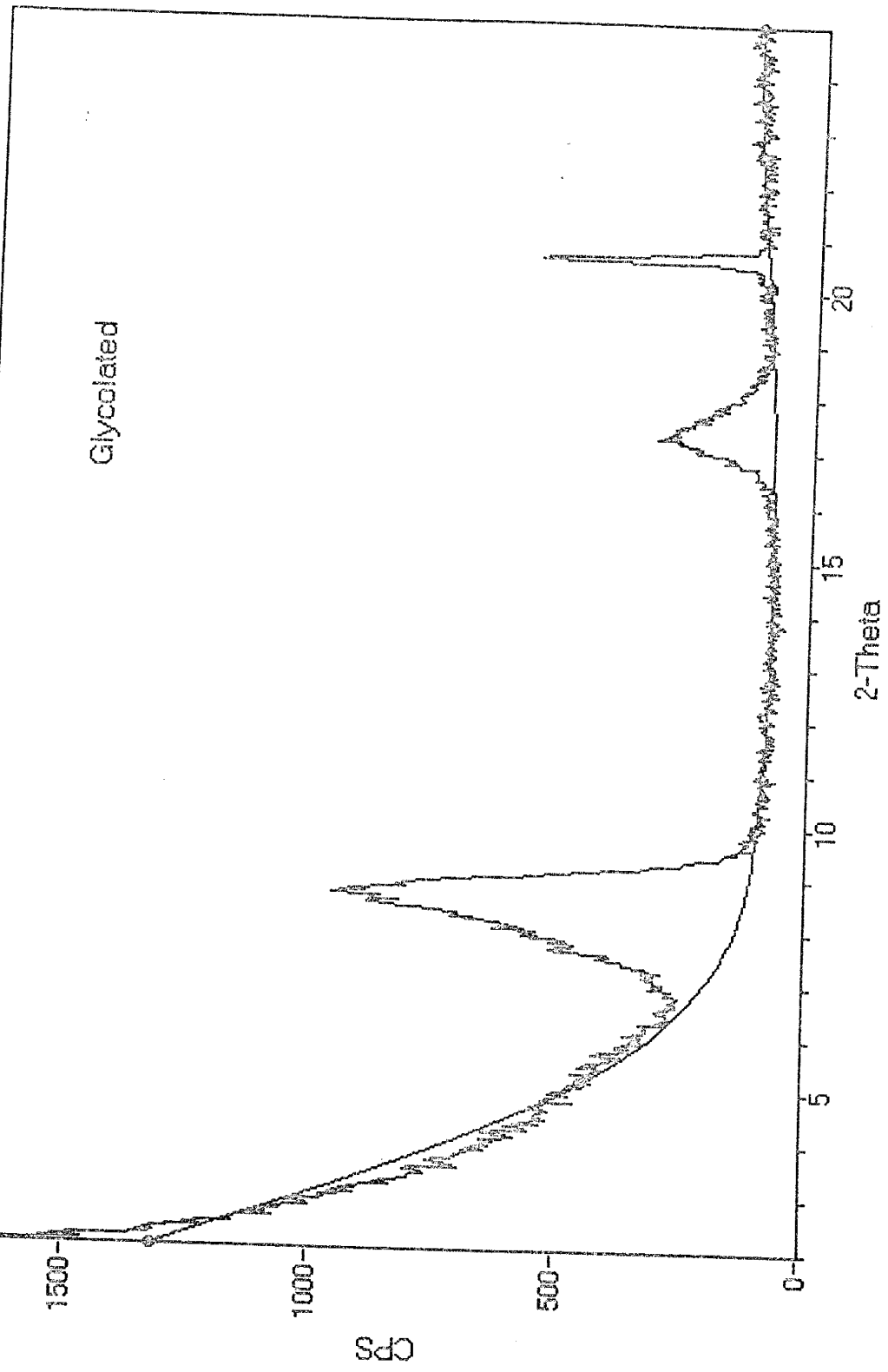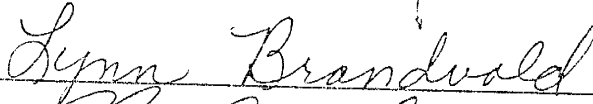
This thesis is accepted on behalf of the faculty
of the Institute by the following committee:

_____
                    Adviser

_____

_____
          Lynn Brandvold

_____

_____

              4/24/98
_____
                    Date